De novo assembly of a PML nuclear subcompartment occurs via multiple pathways and induces telomere elongation

Inn Chung [1], Heinrich Leonhardt [2] and Karsten Rippe [1]*

[1] German Cancer Research Center & BioQuant, Research Group Genome Organization & Function, Im Neuenheimer Feld 280, 69120 Heidelberg, Germany

[2] Department of Biology II, Center for Integrated Protein Science, Ludwig Maximilian University Munich, 82152 Planegg-Martinsried, Germany

* to whom correspondence should be addressed

E-mail: Karsten.Rippe@dkfz.de; Tel.: +49-6221-5451376; Fax: +49-6221-54-51487

Running title: Assembly of functional APBs

Keywords: Alternative Lengthening of Telomeres/ DNA repair and recombination / Promyelocytic Leukemia Nuclear Bodies

Summary

Telomerase-negative tumor cells use an alternative lengthening of telomeres (ALT) pathway that involves DNA recombination/repair to maintain their proliferative potential. The cytological hallmark of this process is the accumulation of promyelocytic leukemia (PML) nuclear protein at telomeric DNA to form ALT associated PML bodies (APBs). Here, the de novo formation of APBs was investigated by tethering its putative protein components to telomeres. We show that functionally distinct proteins were able to initiate APB formation with high efficiency in a self-organizing and self-propagating manner. These included (i) PML and Sp100 as the constituting components of PML nuclear bodies, (ii) the telomere repeat binding factors TRF1 and TRF2, (iii) the DNA repair factor NBS1, and (iv) SUMO E3 ligase MMS21 as well as the isolated SUMO1 domain via an interacting domain of another protein factor. In contrast, repair factors Rad9, Rad17 and Rad51 were less efficient in APB nucleation but are recruited to preassembled APBs. The artificially created APBs induce telomeric extension via a DNA repair mechanism as inferred from their co-localization with non-replicative DNA synthesis and H2A.X phosphorylation and an increase of the telomere repeat length. These activities were absent after recruitment of APB factors to a pericentric locus and establish APBs as functional intermediates of the ALT pathway.

Introduction

Telomeres, the ends of the linear chromosomes, contain repetitive DNA sequences (in humans $(TTAGGG)_n$, typically 3 to 20 kb in length) that are organized into a specialized nucleoprotein complex. This structure protects the telomeres from being processed as a DNA double-strand break by the DNA repair and recombination machinery of the cell (de Lange et al., 2006; Verdun and Karlseder, 2007). Telomeres shorten with every cell division due to the incomplete replication of the lagging strand and additional exonucleolytic activities. Upon reaching a critical length cellular senescence is induced (Collado et al., 2007). In most tumor cells the reverse transcriptase telomerase is reactivated that is able to extend the telomere repeat sequences for unlimited proliferation. However, some immortalized cell lines and 10 - 15% of cancer cells use an alternative lengthening of telomeres (ALT) mechanism for the maintenance of their telomere repeats (Henson et al., 2002). This pathway involves DNA repair and recombination processes (Dunham et al., 2000). ALT-positive cells are characterized by the association of telomeric DNA with promyelocytic leukemia nuclear bodies (PML-NBs) forming ALT associated PML-NBs (APBs) (Henson et al., 2002). PML-NBs are mobile nuclear subcompartments present in most mammalian cells and have been implicated in a variety of cellular functions including apoptosis, senescence, tumor suppression, transcription, antiviral response or DNA replication and repair (Bernardi and Pandolfi, 2007; Dellaire and Bazett-Jones, 2004; Lallemand-Breitenbach and de The, 2010; Takahashi et al., 2004). APBs co-localize with DNA repair and recombination proteins, and a number of models for the molecular mechanisms have been proposed to explain the role of APBs in the ALT pathway (Cesare and Reddel, 2010; Draskovic et al., 2009; Henson et al., 2002; Jiang et al., 2007). However, it is not clear whether a functional link between APB formation and telomere lengthening exists. To address this issue we investigated the de novo formation of APBs. Protein components of APBs were recruited to telomeres tagged with stable integrations of bacterial *lac* operator DNA sequence (*lac*O) repeats in the ALT-positive human osteosarcoma U2OS cell line (Jegou et al., 2009). This system allows the elucidation of the APB assembly process after enriching one factor and the dissection of the interaction network that leads to APB formation and the recruitment of DNA repair and recombination factors. Furthermore, we show that the de novo formation of APBs induces the elongation of telomeric repeats in a DNA repair based synthesis process. This

demonstrates that APBs are indeed functional intermediates in the ALT pathway and identifies them as potential targets for the treatment of ALT-positive tumors.

Results

Recruitment of PML and Sp100 to *lac*O labeled telomeres leads to the assembly of de novo APBs

The ALT-positive U2OS cell line F6B2 that has three stable integrations of bacterial *lac* operator (*lac*O) repeats adjacent to the telomeres of chromosomes 6q, 11p and 12q (Jegou et al., 2009) was transfected with a bacterial LacI repressor fused to a GFP-binding protein (GBP) (Deng et al., in preparation; Rothbauer et al., 2006; Zolghadr et al., 2008). The LacI construct with (GBP-LacI-RFP) or without (GBP-LacI) an additional red fluorescent mRFP1 marker was used to recruit GFP (or YFP) tagged proteins and interacting factors to the telomere associated *lac*O arrays (Fig. 1 A). As described in previous studies, the GBP domain binds with high affinity to GFP with an equilibrium dissociation constant of 0.23 nM (Rothbauer et al., 2006). Thus, this system is equivalent to the use of direct fusion constructs of LacI with the protein of interest (e.g. (Kaiser et al., 2008; Soutoglou and Misteli, 2008; Tumbar et al., 1999)). Accordingly, the recruitment of GFP-PML via GBP-LacI-RFP in the F6B2 cell line results in co-localization of GFP-PML with the three telomeres (Fig. 1 B). In order to address whether tethering PML to the *lac*O labeled telomeres leads to the assembly of APB-like structures at these sites, the presence of the main structural components of PML-NBs was analyzed. For this, we used the PML III splicing variant that itself appears to have no specific interactions with shelterin proteins as opposed to PML IV (corresponding to PML 3 in the arabic numbering scheme), for which binding to TRF1 was reported (Yu et al., 2009). While PML IV showed a similar behavior in control experiments (data not shown), the use of PML III allowed us to separate the initial telomeric recruitment event (provided in our system by *lac*O/GBP-LacI) more clearly from other protein-protein interactions of PML.

PML-NBs are composed of PML and Sp100 proteins that carry post-translational SUMO (small ubiquitin-like modifier) modifications and organize in a spherical shell (Bernardi and Pandolfi, 2007; Lang et al., 2010; Shen et al., 2006). Accordingly, we investigated whether PML or Sp100 recruitment would result in the accumulation of other components (Fig. 2). GFP tagged PML protein was efficiently bound to the *lac*O arrays via GBP-LacI-RFP. This triggered the subsequent recruitment of endogenous Sp100 to these sites with an efficiency of 100 % (Fig. 2 A). The reverse experiment, tethering GFP-Sp100 to the *lac*O arrays, also

induced the formation of APBs since endogenous PML was detected at all GFP-Sp100 positive *lac*O arrays (Fig. 2 B). Furthermore, the recruitment of GFP-PML increased the presence of endogenous SUMO isoforms to more than 90 % (93 ± 9 % for SUMO1, 98 ± 11 % for SUMO2/3, Fig. 2 C, D). In contrast, transfection of only GBP-LacI-RFP or GBP-LacI-RFP together with the isolated GFP domain did not lead to a significant enrichment of endogenous PML or Sp100 at these sites (Fig. 2 E and Fig. S1 A). Likewise, co-transfecting RFP-LacI without the GBP domain together with GFP-PML did not target PML to the *lac*O arrays (data not shown). The residual degree of co-localization in the control cells is likely to reflect the presence of endogenously formed APBs at the three tagged telomeres, as well as random superposition of the two signals in the same optical section of the confocal images. Together, our results indicate that the artificial enrichment of GFP-PML at those telomeres leads to the assembly of bona fide APBs (defined as PML-NBs at telomeres) with respect to their structural composition. This is further supported by the enlarged view of the artificially formed APBs that revealed the accumulation of PML and Sp100 around the telomeres in a structure that was indistinguishable from endogenous APBs imaged previously (Fig. S1 B) and the other experimental findings given below (Jegou et al., 2009; Lang et al., 2010).

SUMO1 interactions are essential for APB assembly

Since impairment of sumoylation disrupts PML-NB formation and sumoylated telomeric proteins are crucial for the formation of APBs in ALT-positive cells (Potts and Yu, 2007; Shen et al., 2006), we investigated the effect of tethering the SUMO domain to the *lac*O tagged telomeres. Recruiting GFP-SUMO1/2/3 constructs was clearly sufficient for initiating APB formation as judged from co-localizations of 80-85 % (presence of endogenous PML, Fig. 3 A-C), 60-80 % (presence of endogenous Sp100, Fig. S2 A-C) and 40-50 % (presence of endogenous Rad17, Fig. S2 D-F). APB proteins like PML and Sp100 are subject to sumoylation and, at the same time, contain SUMO-interacting motifs (SIM) (Hecker et al., 2006; Knipscheer et al., 2008; Shen et al., 2006). Thus, in these experiments the effect of GFP-SUMO that was covalently conjugated to its target proteins and non-covalent interactions via the SIMs could not be distinguished (Fig. S3). Accordingly, we investigated SUMO constructs that could not be conjugated to other proteins. The covalent attachment of

SUMO occurs via cleavage of its C-terminus exposing a gly-gly motif that becomes bound to a lysine residue of the target protein (Geiss-Friedlander and Melchior, 2007; Muller et al., 2001). The YFP-SUMO1ΔC7, GFP-SUMO2ΔC4 and the GFP-SUMO3ΔC13 mutants that lack the C-terminal double glycine motif can no longer be attached to target proteins (Ayaydin and Dasso, 2004; Lin et al., 2006; Mukhopadhyay et al., 2006). Tethering the SUMO1ΔC7 mutant to the *lac*O labeled telomeres resulted in APB formation with an efficiency that was similar to that of the conjugable wild type SUMO1 construct (77 ± 6 % versus 82 ± 10 % co-localization with endogenous PML, Fig. 3 A, D). Thus, the interaction of an isolated SUMO1 domain with the SIMs of other proteins is sufficient for the APB nucleation event. In contrast, the non-conjugable mutants of SUMO2 and SUMO3 were significantly less efficient in this respect, yielding co-localization with endogenous PML of 46 ± 5 % (GFP-SUMO2ΔC4) and 45 ± 7 % (GFP-SUMO3ΔC13) (Fig. 3 E, F). To test whether SIM-SUMO1 interactions are indeed essential for the de novo APB assembly, the YFP-SUMO1ΔC7(-) variant was evaluated. It was constructed by changing the amino acids Val38 and Lys39 to alanines. These residues are part of the second β-strand of SUMO1, which is crucial for SIM binding as shown in several studies, e.g. (Perry et al., 2008; Song et al., 2005). Accordingly, YFP-SUMO1ΔC7(-) can neither be conjugated to another protein nor bind to a SIM. As shown in Fig. 3 G, tethering this construct to the telomeres did not increase co-localization with endogenous PML over background levels. Thus, a SIM interaction with SUMO1 is a central component of APB nucleation. This conclusion is in line with the behavior of yet another type of SUMO construct, namely a C-terminally tagged GFP fusion of SUMO3 (Fig. 3 H). This fusion protein appeared to be mostly resistant to cleavage of the C-terminus during the maturation process since it was not conjugated (Fig. S3). Interestingly, this variant was also unable to induce *de novo* APB assembly upon telomere recruitment, which might be due to interference of the C-terminal GFP-tag with SIM binding.

De novo APB formation can be induced with high efficiency by recruiting the shelterin components TRF1 and TRF2 and recombination factor NBS1, but not Rad9, Rad51 or Rad17

Other known APB components were tested for their capability of inducing the assembly of PML-NBs when recruited to telomeres. First, the telomere repeat binding factors TRF1 and

TRF2 were investigated (Fig. 4 A, B). Both TRF1 and TRF2 bind to telomeric repeats and are therefore present in endogenous APBs. Tethering these factors resulted in a strong increase of co-localization with endogenous PML, with TRF2 being somewhat more efficient than TRF1 (85 ± 7 % co-localization with GFP-TRF2 and 70 ± 8 % with GFP-TRF1, Fig. 4 A, B).
Since APBs are characterized by the presence of several DNA repair and recombination proteins, the propensity of such proteins to drive APB assembly was examined. The recombination factors NBS1 and Rad51, as well as the DNA repair factors Rad9 and Rad17 were tethered to the *lac*O arrays as GFP fusions (Fig. 4 C-F, Table 1). Recruitment of NBS1, which is a central component of the MRN (Mre11/Rad50/NBS1) repair/recombination complex, increased endogenous PML levels at the *lac*O telomeres with a high efficiency to 83 ± 9 % (Fig. 4 C) (Jiang et al., 2005; Jiang et al., 2007; Wu et al., 2003). Rad51 is a central player in DSB repair via homologous recombination and is also involved in normal telomere function, presumably by promoting t-loop formation (Verdun and Karlseder, 2007; West, 2003). Furthermore, Rad51 is present in APBs (Yeager et al., 1999). The recruitment of GFP tagged Rad51 led only to a small increase of endogenous PML at these telomeres to 40 ± 4 % (Fig. 4 D). The Rad9 and Rad17 proteins are part of the RFC-Rad17/9-1-1 complex that participates in DNA damage response, plays a role in telomere stability and is a component of APBs (Nabetani et al., 2004; Pandita et al., 2006; Parrilla-Castellar et al., 2004). Enriching GFP-Rad9 at the *lac*O labeled telomeres resulted in subsequent recruitment of endogenous PML with an efficiency of 59 ± 6 % (Fig. 4 E). In contrast to the other investigated proteins, recruitment of GFP-Rad17 did not initiate the assembly of PML-NBs (Fig. 4 F).

The composition of de novo APBs is indistinguishable from endogenous APBs

To assess whether the de novo assembled APBs also contain endogenous proteins involved in DNA repair and recombination, we investigated their composition by immunostaining (Fig. 5, Table 1). NBS1, Rad17, Rad9 – all bona fide components of functional APBs (Jiang et al., 2007; Jiang et al., 2009; Nabetani et al., 2004; Wu et al., 2003) – were enriched between two-fold (NBS1, Fig. 5 A) to about four-fold (Rad9, Fig. 5 B) after GFP-PML recruitment. Thus, our de novo assembly approach results in APBs that are functional in terms of their protein composition by all criteria reported in the literature.

APB components can be assembled efficiently at a pericentric *lac*O integration site by targeting PML, TRF1, TRF2 or NBS1 to this locus

In order to examine whether the assembly of APB proteins requires the telomeric location of the *lac*O array, the U2OS cell clone F42B8 was investigated that has one *lac*O array insertion at the pericentric region of chromosomes 2p (Fig. S4) (Jegou et al., 2009). These cells showed a higher level of co-localization of endogenous PML with the *lac*O arrays (44 ± 6 %) as compared to the telomeric *lac*O sequences (Fig. S5 A). This is in line with previous reports that described the co-localization of PML-NBs with pericentric heterochromatin (Everett et al., 1999; Luciani et al., 2006). Recruiting GFP-PML to the pericentric *lac*O array led to a similar enrichment of endogenous SUMO isoforms indicating an assembly mechanism that is independent of the chromosomal site (Fig. S5 B, C). Furthermore, TRF1 and TRF2 were similarly efficient in the subsequent recruitment of endogenous PML to the pericentric locus as they were at telomeric sites (Fig. 4 A, B, Fig. S6 A, B). A comparable result was obtained when tethering NBS1 to the pericentric *lac*O array (Fig. S6 C), while GFP tagged Rad51 could not initiate PML-NB formation at this locus (Fig. S6 D). We then tested whether the accumulation of endogenous APB marker proteins at pericentric regions upon GFP-PML recruitment was different. Remarkably, the protein composition of the nuclear bodies induced by recruitment of GFP-PML to the pericentric *lac*O arrays revealed that all factors are enriched under these conditions to a similar or even higher degree than at the telomeric sites (Fig. 5, right panel). Thus, the de novo assembled nuclear bodies at the pericentric chromatin locus had an APB-like protein composition.

APB assembly can be induced by the MMS21 SUMO E3 ligase and occurs in two steps

The SUMO E3 ligase MMS21 induces the sumoylation of several telomere repeat-associated proteins like TRF1, TRF2, and Rap1 in ALT-positive cells and thereby supports APB formation (Potts and Yu, 2007). In order to investigate the role of MMS21, we first tested for the presence of endogenous MMS21 at the *lac*O labeled telomeres after GFP-PML recruitment (Fig. 6 A). MMS21 was highly enriched upon tethering PML at these sites resulting in an increase of co-localization from 19 ± 3 % to 68 ± 7 %. Interestingly, the

nuclear bodies formed de novo at the pericentric *lac*O array contained endogenous MMS21 at similar levels (79 ± 9 % as opposed to 28 ± 5 % in the GFP control, Fig. 6 B).

Next, we sought to test whether the presence of MMS21 at telomeres is sufficient to initiate APB formation. To this end, GFP-MMS21 was recruited to the telomeric *lac*O sequences. We observed that GFP-MMS21 is highly efficient in promoting APB assembly as it increased co-localization with endogenous PML from 19 ± 5 % to 86 ± 9 % (Fig. 6 C). Notably, tethering the GFP-MMS21 to the pericentric *lac*O sites also increased the co-localizing endogenous PML from 44 ± 6 % to 95 ± 10 %, which suggests that other sumoylation targets/interaction partners might exist in addition to telomere-associated proteins (Fig. S6 E). Next, we addressed the question whether the GFP-MMS21 induced targeting of endogenous PML protein to the telomeric *lac*O sites was accompanied by the enrichment of the DNA repair factor Rad9. The enrichment of endogenous PML and Rad9 at these sites was evaluated by immunofluorescence (Fig. 6 D). Remarkably, 35 ± 4 % of the GFP-MMS21 bound telomeres co-localizing with PML did not contain Rad9 (Fig. 6 D1, D3, E). In contrast, no co-localization of endogenous Rad9 with GFP-MMS21 was detected without the simultaneous presence of PML. To compare this result with native APBs we investigated the PML/Rad9 ratio at telomere repeats identified via GFP-TRF2. The vast majority of endogenous APBs (defined as co-localization of PML and TRF2) contained both proteins. Only 2 % of the telomeres with PML did not contain Rad9 and only 0.9 % of the TRF2-Rad9 co-localization had no PML (Fig. 6 E). On average, we detected 54 ± 11 telomeres per cell of which 8 ± 3 were associated with APBs. Endogenous APBs were found in almost every cell of the asynchronous cell population in contrast to previous reports (Yeager et al., 1999). It is noted that our CLSM based detection included also relatively small co-localization spots as discussed in further detail elsewhere (Osterwald et al., 2011). In summary, the fully assembled functional endogenous APBs contain both PML and Rad9, which is in line with previous work showing PML co-localizing with almost all Rad9 foci in U2OS cells (Nabetani et al., 2004). In the de novo assembly process initiated by recruitment of GFP-MMS21, however, a two-step process was revealed: Tethering MMS21 to the telomere led to the concomitant assembly of the PML/Sp100/SUMO network, presumably via sumoylation of target proteins. Subsequently the DNA recombination/repair factor Rad9 protein was

recruited as apparent from the 35 ± 4 % fraction of GFP-MMS21 co-localization with endogenous PML that did not contain endogenous Rad9 (Fig. 6 D, E).

Recruitment of PML induces DNA repair synthesis at telomeric but not at pericentric sites

Since the ALT mechanism involves DNA double-strand break repair and recombination processes, it was investigated whether the de novo assembled APBs induced these activities. First, we probed de novo formed APBs for the presence of the phosphorylated form of the histone variant H2A.X (γH2A.X), a molecular marker for double-strand break repair and component of APBs (Cesare et al., 2009; Ismail and Hendzel, 2008; Nabetani et al., 2004). Indeed, an 11 ± 7 % higher γH2A.X co-localization was found, which is indicative of an increased activity in DNA double-strand break repair processes (Fig. 7 A). In contrast, no significant enrichment of the γH2A.X signal was detected when GFP-PML was tethered to the pericentric *lac*O arrays (Fig. 7 A, right panel).

Second, we tested for non-replicative DNA synthesis with a 5-bromo-2-desoxyuridine (BrdU) pulse labeling after transfection of the cells with GBP-LacI-RFP and GFP-PML and subsequent staining with an α-BrdU antibody. To differentiate the > 50 replication foci that occur during S-phase in U2OS cells from the sites of non-replicative DNA synthesis, we evaluated only those cells that displayed ≤ 3 BrdU foci (Nabetani et al., 2004). In agreement with previous reports that addressed DNA synthesis in APBs (Wu et al., 2000), the analysis of the BrdU incorporation pattern revealed a clear increase of non-replicative DNA synthesis at the telomeres at the sites of de novo formed APBs by 11 ± 5 % as compared to the control cells, where only endogenously formed APBs were present (Fig. 7 B). Again, this increase was not observed after recruitment of PML to the pericentric *lac*O integration where the fraction of co-localizing BrdU signal did not significantly differ from the background level (Fig. 7 B, right panel). Together, these results indicate that the de novo assembled nuclear bodies consist of an APB-like protein composition independent of the chromosomal site of assembly. However, they have to be assembled at telomeres to induce DNA repair process as detected here by H2A.X phosphorylation and BrdU incorporation.

De novo APBs induce telomere repeat extension

In order to directly evaluate changes in telomere repeat length associated with de novo APB formation, fluorescence in situ hybridization (FISH) with a PNA probe against the telomere repeat sequence was conducted (Fig. 8) (Jegou et al., 2009). Due to the heterogeneity of telomere repeat length in ALT-positive cells a significant amount of the chromosomal ends is too short to display a detectable telomere repeat PNA signal. The fraction of these telomeres was determined at several time points after transfecting F6B2 cells with GBP-LacI and either GFP-PML or a GFP only control. The recruitment of GFP-PML to the telomeric *lac*O arrays led to an increase of the detectable TTA$(G)_3$ signal at these sites that increased over time from 57 ± 7 % (12 h) up to 81 ± 9 % (96 h after transfection). In these experiments, a telomere signal was counted if it comprised >0.025 % of the total PNA intensity in a given nucleus (Fig. 8 B, left panel). The telomere repeats were also examined at the pericentric *lac*O arrays. Notably, there was no significant change of the telomeric repeat signal when GFP-PML was recruited to this site (Fig. 8 B, right panel). This suggests that the observed increase of the TTA$(G)_3$ signal at the *lac*O labeled telomeres can be indeed attributed to an extension of the telomere repeats at the tagged telomere as opposed to the association with the telomere of another chromosome only due to the induced accumulation of PML protein. Then a quantitative analysis of the TTA$(G)_3$ signal intensity distribution was conducted. This revealed the appearance of a ~20 % fraction of telomeres with an increased normalized repeat length of 3.4 ± 0.8 % when GFP-PML was targeted to the telomeres (Fig. 8 C). Finally, the images were inspected to determine whether the increase of telomere repeat signal at the de novo formed APBs was due to an induction of clustering of two or more telomeres. Only 2 out of 604 or 0.3 % of the complexes showed a telomere intensity signal distribution indicative of the presence of two telomeres.

Discussion

Here, we have investigated the assembly mechanism of APBs and their function in the ALT pathway by recruiting protein components of APBs to *lac*O labeled telomeres in U2OS cells (Fig. 1). As described previously, the structure of the PML-NB component of APBs is determined by PML and Sp100 proteins in conjunction with their sumoylation to mediate the non-covalent binding of the two proteins via their SUMO interacting motifs (SIMs) (Fig. 2) (Bernardi and Pandolfi, 2007; Lang et al., 2010; Shen et al., 2006).

The shelterin components TRF1 and TRF2 were highly capable of inducing the formation of de novo APBs after enrichment at the telomeric *lac*O arrays (Fig. 4 A, B). This is consistent with their requirement for APB formation from previous reports (Jiang et al., 2007). The results obtained here suggest that the amount of TRF1/2 accessible to protein-protein interactions or post-translational modifications, particularly sumoylation, can be a limiting factor for APB assembly at endogenous telomeres. It is noted that the recruitment of TRF1/2 via the *lac*O arrays allowed us to target also very short telomeres, which presumably lack parts of the shelterin complex. Enrichment of TRF1/2 at these telomeres could provide the required additional interaction surface for APB formation. Surprisingly, TRF2 was somewhat more efficient than TRF1 in recruiting endogenous PML, although a direct interaction between TRF1 and PML IV in the context of APB formation was reported recently (Yu et al., 2009). However, the antibody used here recognizes all PML isoforms so that a specific recruitment of PML IV might not be detected in our assay.

With our experimental system we were able to dissect the role of the three different paralogues SUMO1, 2, and 3 (Fig. 3). Intriguingly, a non-conjugable SUMO1 mutant was found to be highly efficient in triggering the assembly of APB proteins, while mutated SUMO2 and SUMO3 that could not be conjugated to a target protein showed only a moderate propensity to initiate this process. It is speculated that the modification of telomeric proteins with SUMO1 (as mimicked in our experiments by the tethering of a non-conjugable SUMO1 mutant or the MMS21 SUMO E3 ligase) would be sufficient to initiate the formation of an APB via recruitment of SIM containing APB components. This conclusion is further corroborated by our findings that SIM interactions of non-conjugable SUMO1 are crucial for efficient APB nucleation in line with previous reports (Bernardi and Pandolfi, 2007; Shen et al., 2006). Moreover, our recent high-resolution 3D analysis of PML-NBs revealed that the

SUMO1 modification is localized preferentially in the spherical shell of PML and Sp100 protein, whereas the SUMO2/3 modification was found also in the interior of PML-NBs points to functional differences between the isoforms (Lang et al., 2010). Thus, we propose that PML binds SUMO1 directly by its SIM whereas SUMO2 and SUMO3 are more weakly/indirectly bound by the main PML-NB component.

The SUMO1 modification of target proteins as an initiating factor for APB formation could be set by the MMS21 SUMO E3 ligase. This enzyme is responsible for sumoylation of the shelterin components TRF1, TRF2, and Rap1 in ALT cells and can auto-sumoylate itself (Andrews et al., 2005; Potts and Yu, 2005; Zhao and Blobel, 2005). In support of this model, recruitment of MMS21 was found to initiate APB formation as efficiently as the SUMO1 domain (Fig. 3 A, D, 6 C), indicating that MMS21 promotes APB assembly via a recruitment and not a maintenance mechanism (Potts and Yu, 2007). Thus, the stabilization and spreading of the APB protein interaction network could occur via a positive feedback-loop including binding of PML and Sp100 to sumoylated proteins via their SIMs. Surprisingly, tethering MMS21 to the pericentric site was as efficient in accumulation of PML protein as it was at the tagged telomeres (Fig. 6 C, S6 E). This points to additional targets for MMS21-mediated sumoylation apart from telomeric proteins that play a role in PML-NB assembly. In agreement with this view, endogenous MMS21 accumulated after enrichment of PML at these sites (Fig. 6 B). The mutual recruitment of MMS21 and PML could involve the capability of MMS21 to sumoylate itself followed by the SIM directed binding of PML. Interestingly, in addition to MMS21 also the PML protein itself possibly has a SUMO E3 ligase activity that could further amplify this propagation process (Quimby et al., 2006). In agreement with this view, PML-NBs have been described as “hotspots” for sumoylation in the nucleus (Saitoh et al., 2006; Van Damme et al., 2010). Moreover, this model is supported by the observation that APB formation is initiated at the *lac*O arrays in our experiments, but subsequently extends further to include both the *lac*O arrays and the telomere repeats in the de novo formed APBs (Fig. S1 B) (Jegou et al., 2009; Lang et al., 2010).

Investigating the role of DNA recombination and repair factors showed that the recombination protein NBS1 was highly capable of inducing PML binding to telomeres when recruited as a GFP construct (Fig. 4 C). However, the level of endogenous NBS1 was only slightly increased by ~10% over the background in de novo formed APBs (Fig. 5 A). This

clearly distinguishes this protein from the more abundant proteins PML and Sp100. In previous studies interactions of NBS1 with Sp100 and TRF1/2 were found to be required for recruiting DNA repair factors Mre11, Rad50 and Brca1 to APBs (Naka et al., 2002; Wu et al., 2003; Zhu et al., 2000). This process seems to be tightly regulated in the endogenous environment as we observed a higher enrichment of endogenous NBS1 after recruiting GFP-PML to a pericentric site that might lack specific inhibitory mechanisms. In addition to its DNA repair/recombination activity, NBS1 could target PML-NB assembly to certain telomeres at which it is enriched. This might lead to a DSB repair mediated elongation at these sites. Furthermore, the strong accumulation of PML protein after tethering of NBS1 to the pericentric array supports an ALT independent relationship between DSB signaling and PML-NB formation as suggested previously (Dellaire and Bazett-Jones, 2004; Dellaire and Bazett-Jones, 2007). This might be triggered by the persistent deposition of NBS1 on the chromatin mimicking a DNA double-strand break situation (Soutoglou and Misteli, 2008).

The homologous recombination (HR) factor Rad51 plays an important role in HR mediated DSB repair as it forms nucleoprotein filaments on single-stranded DNA to promote the pairing of homologous strands and strand exchange. It was one of the first recombination factors that have been described as APB components in ALT cells (Yeager et al., 1999). Interestingly, recruitment of this factor to the telomeric *lac*O arrays promoted APB formation only weakly (Fig. 4 D). This is consistent with a previous report that siRNA mediated knockdown of Rad51 in U2OS cells does not lead to a disruption of APBs (Potts and Yu, 2007). With respect to the assembly mechanism, this suggests a classification of APB proteins that are capable of initiating the assembly and others that are only recruited subsequently. This accounts also for the results obtained by testing the repair factors Rad9 and Rad17. For these proteins, the accumulation of endogenous proteins in the de novo formed APB was higher (Fig. 5 B, C) than the increase in the level of endogenous PML proteins when GFP-Rad9 and GFP-Rad17 were enriched at the telomeres (Fig. 4 E, F). This suggests that both Rad9 and Rad17 are less efficient as initiation factors for APBs but readily assemble at these sites once these complexes are formed. This view is supported by our finding that Rad9 binding to telomeres correlated with the presence of PML but not vice versa (Fig. 6). It suggests that during endogenous APB formation, the assembly of structural

nuclear body core components PML and Sp100 precedes the subsequent binding of DNA repair and recombination factors.

The comparison of de novo assembled nuclear bodies after recruitment of GFP-PML to a pericentric *lac*O array revealed a self-organization process that was independent of the chromosomal site once PML was enriched: SUMO1/2/3, NBS1, Rad9, Rad17, and MMS21 were found enriched both at the telomeric and the pericentric sites at similar levels. This points to a self-organization process of the examined de novo APBs with stochastic interactions of the constituting components as opposed to a defined sequential order of binding events (Fig. 9) (Dinant et al., 2009; Hancock, 2004; Hebert and Matera, 2000; Matera et al., 2009; Misteli, 2007; Wachsmuth et al., 2008). This aspect of APB formation is very similar to that reported for Cajal nuclear bodies (Kaiser et al., 2008). It is supported by experiments on the dissociation and reassembly of PML-NBs via varying the degree of molecular crowding in their environment (Hancock, 2004).

In addition to previous findings on the self-organizing properties of nuclear bodies we propose that the APB protein interaction network is stabilized by a feedback and propagation mechanism that comprises (i) the MMS21 SUMO E3 ligase and possibly other E3 ligases, (ii) the post-translational sumoylation of PML, Sp100, telomeric proteins TRF1, TRF2, and Rap1, and MMS21 itself, and (iii) the SUMO interacting domains of PML and Sp100 (Fig. 9). In contrast to the initiating proteins, other APB proteins like Rad9, Rad17 and Rad51 are incorporated later in conjunction with phosphorylation of the H2A.X histone variant. Thus, a preassembled subset of APB components is required for the subsequent binding of other factors. This feature of sequential assembly mechanism has been reported previously for the recruitment of Sp100 and Daxx to early G1 PML-NBs and the prior binding of the MRN complex to telomeres before APB assembly (Chen et al., 2008; Jiang et al., 2007).

The APBs assembled here by recruiting essential structural components of APBs like PML, Sp100 and SUMO1 to the telomere-associated *lac*O arrays were indistinguishable from their endogenous counterparts with respect to protein composition and structural organization according to all criteria reported previously. This allowed us to address the question whether this nuclear subcompartment has an essential function within the ALT pathway. To this end, we evaluated the presence of the phosphorylated γH2A.X histone variant as a molecular marker for double-strand break repair as well as non-replicative DNA synthesis via the

incorporation of BrdU into the DNA (Fig. 7). We found that the de novo assembled APBs were positive for these two hallmarks of DNA repair. Presumably these activities are coupled to the DNA damage response pathway, as previous work has shown that BrdU incorporation in APBs is dependent on the PI-3-kinase-like kinases ATR and ATM (Nabetani et al., 2004). Finally, we showed by quantitative FISH that the recruitment of GFP-PML to the telomeric *lac*O arrays led to an increase of the telomere repeat length at these sites (Fig. 8). A fraction of 10-15 % of the de novo formed APBs was competent in inducing telomere extension during a ~24 h time period. This number is consistent with the result that not all of the de novo APBs contained the complete set of DNA repair/recombination factors investigated here (Fig. 5, Table 1). Longer incubation of the cells further increased the percentage of functional APBs to a ~30 % fraction of APBs with telomere extension activity after 96 h (Fig. 8 A, left panel). As discussed above, recruitment of PML to a non-telomeric site led to the formation of a nuclear body that contained all tested APB proteins. However, this nuclear subcompartment was non-functional with respect to H2A.X phosphorylation and the non-replicative synthesis of telomeric DNA as there was no significant difference in BrdU incorporation and the detected telomere repeat signal (Fig. 7, Fig. 8 B).

Previously, it was proposed that APBs promote the association of multiple telomeres (Draskovic et al., 2009) or the binding of extrachromosomal telomeric repeat DNA after induction of DNA damage (Fasching et al., 2007). Our structural analysis of endogenous and de novo assembled APBs by conventional CLSM and high-resolution 4Pi microscopy revealed a cap like structure of PML protein around a single telomere end in the U2OS cell line (Fig. 1 B) (Jegou et al., 2009; Lang et al., 2010). Only for a fraction of 0.3% of the APBs evaluated here that formed after PML recruitment two telomere signals could be distinguished. For endogenous APBs this number was even smaller at about 0.1%. This conclusion is supported by an advanced automated 3D image analysis of confocal 3D stacks of endogenous APBs in U2OS cells visualized by immunostaining against PML and TRF2 (Osterwald et al., 2011; Wörz et al., 2010). In this analysis only 6 out of 5803 or 0.1 % of the APBs showed two distinguishable telomere signals. Thus, under our experimental conditions we did not find evidence that telomere clustering could explain the observed increase of the telomere repeat signal at the de novo formed APBs. Furthermore, the experiments with the pericentric *lac*O arrays demonstrated that recruiting APB proteins to a non-telomeric locus

did not lead to binding of other telomeres or extrachromosomal telomeric repeat DNA, although all APB marker proteins were present (Fig. 8 B). Since the assembly of APB proteins induced H2A.X phosphorylation and BrdU incorporation only at the telomeric sites we conclude that the de novo formation of APBs promotes the extension of the telomere repeat sequence by an intra-telomeric DNA repair synthesis process similar to previously proposed models (Cesare and Reddel, 2010; Henson and Reddel, 2010; Tarsounas and West, 2005). This activity interconnects APBs with the central function in the ALT pathway, and makes them a promising target for therapeutic interventions in ALT-positive tumors. We anticipate that our experimental approach will be helpful to further dissect the exact combination of protein factors that is sufficient to trigger telomere extension in APBs. This will serve to select optimized protein targets for inhibiting telomere extension and cell proliferation in tumors that make use of the ALT pathway.

Materials and Methods

Protein constructs

The cDNAs encoding TRF1, SUMO1, SUMO2, SUMO3, MMS21, Rad51, Rad9 and Rad17 were obtained from the DKFZ Genomics and Proteomics Core Facility and cloned into pcDNA-DEST53 (N-terminal GFP-tag) and pcDNA-DEST47 (C-terminal GFP-tag) expression vectors (Invitrogen). Constructs for GFP-PML III and GFP-TRF2 were described previously (Jegou et al., 2009). The other constructs were kindly provided as indicated: GFP-PML IV (Peter Hemmerich, FLI Jena, Germany, (Weidtkamp-Peters et al., 2008)), GFP-CenpA, (Stephan Diekmann, FLI Jena, Germany (Hemmerich et al., 2008)), GFP-Sp100 and NBS1-2GFP (Thomas Hofmann, DKFZ Heidelberg, Germany), pEYFP-SUMO1ΔC7 (Frauke Melchior, ZMBH Heidelberg, Germany). The non-SIM interacting mutant pEYFP-SUMO1ΔC7(-) was created by site-directed mutagenesis of Val38 and Lys39 to alanines. Non-conjugable GFP-SUMO2ΔC4 and GFP-SUMO3ΔC13 constructs were created from the corresponding pcDNA-DEST53-SUMO2/3 vectors by site-directed mutagenesis replacing the first glycine codon of the C-terminal gly-gly-motif by a stop codon. The fluorescence three-hybrid system for recruiting GFP tagged proteins to *lac*O arrays via GBP-LacI and GBP-LacI-RFP was provided by Chromotek (Munich, Germany).

Cell culture work, immunostaining, and PNA FISH

The U2OS cell clones F6B2 and F42B8 were cultured and transfected as described previously (Jegou et al., 2009). Cells were fixed typically 24 h after transfection with 4 % paraformaldehyde in PBS buffer. For the analysis by immunostaining, cells were washed and permeabilized for 5 min with ice cold 0.1 % (v/v) Triton X100 solution in PBS. After three PBS washes, cells were blocked for at least 15 min with 10 % goat serum in PBS, the solution was removed, and the cells were incubated with appropriate dilutions of specific antibodies against γH2A.X (1:100, rabbit, Millipore), NBS1 (1:200, NB100-143, Novus Biologicals), PML (1:150, PG-M3, Santa Cruz), Rad9 (1:100, M-389, Santa Cruz), Rad17 (1:200, H-300, Santa Cruz), Sp100 (1:200, AB1380, Chemicon), SUMO1 (1:100, FL-101, Santa Cruz) or SUMO2/3 (1:200, rabbit, Abcam). For immunofluorescence of MMS21, cells were fixed with 1 % paraformaldehyde, permeabilization and blocking was conducted in 0.2 % (v/v) Triton X100/

3 % BSA in PBS for 20 min, and the antibody was incubated in the same buffer (1:75, Abnova, NSMCE2 MaxPab, B01). For 5-bromo-2-deoxyuridine (BrdU) staining, cells were seeded, transfected and incubated for 1 or 2 days. Then 100 µM BrdU (Sigma-Aldrich) was added to the medium for 2 to 4 h, the cells were fixed, permeabilized with 0.2 % (v/v) Triton X100/PBS, denatured with 1.5 N HCl for 30 minutes and then stained with an antibody against BrdU (1:50, B44, BD Biosciences). After incubation with primary antibodies the coverslips were washed with PBS containing 0.002 % (v/v) NP40. The appropriate secondary antibodies conjugated to Alexa 488 or Alexa 633 (Molecular Probe) were diluted according to the manufacturer's instructions in PBS, applied to the cells and incubated for 30 to 60 min. After another PBS wash the coverslips were mounted with Vectashield (Vector Laboratories) or Prolong Gold antifade reagent (Molecular Probes) both containing 4',6-diamidino-2-phenylindole (DAPI). For telomere PNA FISH, cells were grown on a slide or coverslip, transfected, incubated for the indicated time, washed with PBS and fixed with 4 % paraformaldehyde. After permeabilization with 0.2 % (v/v) Triton X100/PBS, cells were dehydrated by a series of ethanol washes (70, 85, and 100 % ethanol), air-dried and a Cy3 labeled $(CCCTAA)_3$ PNA probe (Dako, Glostrup, Denmark) was added. Then, samples were denatured at 80 °C for 3 min and hybridization was conducted for at least 3 h at 30 °C. Slides were then washed consecutively with 70 % formamide/10 mM Tris pH 7.4, 2x SSC, 0.1x SSC at 55 °C and 0.05 % Tween-20/ 2x SSC (v/v). In order to enhance the GFP signal, immunofluorescence was conducted as described above using an antibody against GFP (1:500, ab290, Abcam). FISH experiments on metaphase chromosomes were conducted as described before using 200 ng of a Cy3 labeled oligonucleotide probe hybridizing against the *lac*O sequence (Jegou et al., 2009).

Confocal fluorescence microscopy, image analysis and statistical evaluation

Fluorescence images were acquired with a Leica TCS SP5 confocal laser scanning microscope (CLSM). Optical sections with spacing of 0.3 µm along the *z*-axis were recorded. Fluorescence intensities in the different color channels were analyzed on the individual *z*-slices. Cells with appropriate expression levels of the fluorescent cells were chosen. Spots were counted as co-localizing if the signal at the *lac*O array was at least 2-fold above the background and comprised at least 2 pixels with a size of 200 nm. The percentage of *lac*O

arrays with co-localization was determined with the indicated value *n* giving the number of *lac*O arrays evaluated. Error bars were calculated as $\sqrt{n}$, which yields the standard deviation for a Poisson distribution. All experiments were conducted at least three times. In the figures maximum intensity projections of the image stacks are shown. In order to determine whether the percentages of co-localizations after recruiting the proteins of interest were significantly different from the ones obtained in the controls, the Fisher's exact test was used to calculate p-values.

Western blot

5 x 10^6 F6B2 cells were seeded and transfected with GFP-SUMO3 or SUMO3-GFP, incubated for 24 h, washed with PBS, incubated with ice cold RIPA buffer for 30 min at 4°C and centrifuged at 4°C. The supernatant was loaded on a 12% SDS polyacrylamide gel and after blocking with 3% BSA/PBS subjected to western blot analysis with an antibody against GFP (ab290, Abcam) according to the manufacturer's protocol.

Acknowledgements

We are grateful to Ulrich Rothbauer, Kourosh Zolghadr, Thomas Hofmann, Jiri Bartek, Frauke Melchior, Peter Hemmerich and Stephan Diekmann for reagents and help, and Sarah Osterwald, Daniel Parisotto, Jan-Philipp Mallm, Maiwen Caudron-Herger and Thomas Höfer for discussions. This work was supported by the project EpiSys within the BMBF SysTec program.

References

Andrews, E. A., Palecek, J., Sergeant, J., Taylor, E., Lehmann, A. R. and Watts, F. Z. (2005). Nse2, a component of the Smc5-6 complex, is a SUMO ligase required for the response to DNA damage. *Mol Cell Biol* **25**, 185-96.

Ayaydin, F. and Dasso, M. (2004). Distinct in vivo dynamics of vertebrate SUMO paralogues. *Mol Biol Cell* **15**, 5208-18.

Bernardi, R. and Pandolfi, P. P. (2007). Structure, dynamics and functions of promyelocytic leukaemia nuclear bodies. *Nat Rev Mol Cell Biol* **8**, 1006-16.

Cesare, A. J., Kaul, Z., Cohen, S. B., Napier, C. E., Pickett, H. A., Neumann, A. A. and Reddel, R. R. (2009). Spontaneous occurrence of telomeric DNA damage response in the absence of chromosome fusions. *Nat Struct Mol Biol* **16**, 1244-51.

Cesare, A. J. and Reddel, R. R. (2010). Alternative lengthening of telomeres: models, mechanisms and implications. *Nat Rev Genet* **11**, 319-30.

Chen, Y. C., Kappel, C., Beaudouin, J., Eils, R. and Spector, D. L. (2008). Live cell dynamics of promyelocytic leukemia nuclear bodies upon entry into and exit from mitosis. *Mol Biol Cell* **19**, 3147-3162.

Collado, M., Blasco, M. A. and Serrano, M. (2007). Cellular senescence in cancer and aging. *Cell* **130**, 223-33.

de Lange, T., Lundblad, V. and Blackburn, E. (2006). Telomeres. *Cold Spring Harbor mongraph series*.

Dellaire, G. and Bazett-Jones, D. P. (2004). PML nuclear bodies: dynamic sensors of DNA damage and cellular stress. *Bioessays* **26**, 963-77.

Dellaire, G. and Bazett-Jones, D. P. (2007). Beyond repair foci: subnuclear domains and the cellular response to DNA damage. *Cell Cycle* **6**, 1864-72.

Dinant, C., Luijsterburg, M. S., Höfer, T., Von Bornstaedt, G., Vermeulen, W., Houtsmuller, A. B. and van Driel, R. (2009). Assembly of multi-protein complexes that control genome function. *Journal of Cell Biology* **185**, 21-26.

Draskovic, I., Arnoult, N., Steiner, V., Bacchetti, S., Lomonte, P. and Londono-Vallejo, A. (2009). Probing PML body function in ALT cells reveals spatiotemporal requirements for telomere recombination. *Proceedings of the National Academy of Sciences of the USA* **106**, 15726-15731.

Dunham, M. A., Neumann, A. A., Fasching, C. L. and Reddel, R. R. (2000). Telomere maintenance by recombination in human cells. *Nat Genet* **26**, 447-50.

Everett, R. D., Lomonte, P., Sternsdorf, T., van Driel, R. and Orr, A. (1999). Cell cycle regulation of PML modification and ND10 composition. *J Cell Sci* **112**, 4581-8.

Fasching, C. L., Neumann, A. A., Muntoni, A., Yeager, T. R. and Reddel, R. R. (2007). DNA damage induces alternative lengthening of telomeres (ALT) associated

promyelocytic leukemia bodies that preferentially associate with linear telomeric DNA. *Cancer Research* **67**, 7072-7.

Geiss-Friedlander, R. and Melchior, F. (2007). Concepts in sumoylation: a decade on. *Nat Rev Mol Cell Biol* **8**, 947-56.

Hancock, R. (2004). Internal organisation of the nucleus: assembly of compartments by macromolecular crowding and the nuclear matrix model. *Biol Cell* **96**, 595-601.

Hebert, M. D. and Matera, A. G. (2000). Self-association of coilin reveals a common theme in nuclear body localization. *Mol Biol Cell* **11**, 4159-71.

Hecker, C. M., Rabiller, M., Haglund, K., Bayer, P. and Dikic, I. (2006). Specification of SUMO1- and SUMO2-interacting motifs. *J Biol Chem* **281**, 16117-27.

Hemmerich, P., Weidtkamp-Peters, S., Hoischen, C., Schmiedeberg, L., Erliandri, I. and Diekmann, S. (2008). Dynamics of inner kinetochore assembly and maintenance in living cells. *The Journal of Cell Biology* **180**, 1101-14.

Henson, J. D., Neumann, A. A., Yeager, T. R. and Reddel, R. R. (2002). Alternative lengthening of telomeres in mammalian cells. *Oncogene* **21**, 598-610.

Henson, J. D. and Reddel, R. R. (2010). Assaying and investigating Alternative Lengthening of Telomeres activity in human cells and cancers. *FEBS Lett* **584**, 3800-11.

Ismail, I. H. and Hendzel, M. J. (2008). The gamma-H2A.X: is it just a surrogate marker of double-strand breaks or much more? *Environ Mol Mutagen* **49**, 73-82.

Jegou, T., Chung, I., Heuvelmann, G., Wachsmuth, M., Görisch, S. M., Greulich-Bode, K., Boukamp, P., Lichter, P. and Rippe, K. (2009). Dynamics of telomeres and promyelocytic leukemia nuclear bodies in a telomerase negative human cell line. *Molecular Biology of the Cell* **20**, 2070-2082.

Jiang, W. Q., Zhong, Z. H., Henson, J. D., Neumann, A. A., Chang, A. C. and Reddel, R. R. (2005). Suppression of alternative lengthening of telomeres by Sp100-mediated sequestration of the MRE11/RAD50/NBS1 complex. *Molecular and Cellular Biology* **25**, 2708-21.

Jiang, W. Q., Zhong, Z. H., Henson, J. D. and Reddel, R. R. (2007). Identification of candidate alternative lengthening of telomeres genes by methionine restriction and RNA interference. *Oncogene* **26**, 4635-4647.

Jiang, W. Q., Zhong, Z. H., Nguyen, A., Henson, J. D., Toouli, C. D., Braithwaite, A. W. and Reddel, R. R. (2009). Induction of alternative lengthening of telomeres-associated PML bodies by p53/p21 requires HP1 proteins. *J Cell Biol* **185**, 797-810.

Kaiser, T. E., Intine, R. V. and Dundr, M. (2008). De novo formation of a subnuclear body. *Science* **322**, 1713-7.

Knipscheer, P., Flotho, A., Klug, H., Olsen, J. V., van Dijk, W. J., Fish, A., Johnson, E. S., Mann, M., Sixma, T. K. and Pichler, A. (2008). Ubc9 sumoylation regulates SUMO target discrimination. *Mol Cell* **31**, 371-82.

Lallemand-Breitenbach, V. and de The, H. (2010). PML nuclear bodies. *Cold Spring Harb Perspect Biol* **2**, a000661.

Lang, M., Jegou, T., Chung, I., Richter, K., Udvarhelyi, A., Münch, S., Cremer, C., Hemmerich, P., Engelhardt, J., Hell, S. W. et al. (2010). Three-dimensional structure of promyelocytic leukemia nuclear bodies. *Journal of Cell Science* **123**, 392-400.

Lin, D. Y., Huang, Y. S., Jeng, J. C., Kuo, H. Y., Chang, C. C., Chao, T. T., Ho, C. C., Chen, Y. C., Lin, T. P., Fang, H. I. et al. (2006). Role of SUMO-interacting motif in Daxx SUMO modification, subnuclear localization, and repression of sumoylated transcription factors. *Mol Cell* **24**, 341-354.

Luciani, J. J., Depetris, D., Usson, Y., Metzler-Guillemain, C., Mignon-Ravix, C., Mitchell, M. J., Megarbane, A., Sarda, P., Sirma, H., Moncla, A. et al. (2006). PML nuclear bodies are highly organised DNA-protein structures with a function in heterochromatin remodelling at the G2 phase. *J Cell Sci* **119**, 2518-31.

Matera, A. G., Izaguire-Sierra, M., Praveen, K. and Rajendra, T. K. (2009). Nuclear bodies: random aggregates of sticky proteins or crucibles of macromolecular assembly? *Dev Cell* **17**, 639-47.

Misteli, T. (2007). Beyond the sequence: cellular organization of genome function. *Cell* **128**, 787-800.

Mukhopadhyay, D., Ayaydin, F., Kolli, N., Tan, S. H., Anan, T., Kametaka, A., Azuma, Y., Wilkinson, K. D. and Dasso, M. (2006). SUSP1 antagonizes formation of highly SUMO2/3-conjugated species. *J Cell Biol* **174**, 939-49.

Muller, S., Hoege, C., Pyrowolakis, G. and Jentsch, S. (2001). SUMO, ubiquitin's mysterious cousin. *Nat Rev Mol Cell Biol* **2**, 202-10.

Nabetani, A., Yokoyama, O. and Ishikawa, F. (2004). Localization of hRad9, hHus1, hRad1, and hRad17 and caffeine-sensitive DNA replication at the alternative lengthening of telomeres-associated promyelocytic leukemia body. *J Biol Chem* **279**, 25849-57.

Naka, K., Ikeda, K. and Motoyama, N. (2002). Recruitment of NBS1 into PML oncogenic domains via interaction with SP100 protein. *Biochem Biophys Res Commun* **299**, 863-71.

Osterwald, S., Wörz, S., Reymann, J., Sieckmann, F., Rohr, K., Erfle, H. and Rippe, K. (2011). A three-dimensional co-localization RNA interference screen platform to elucidate the alternative lengthening of telomeres pathway. *Biotechnology Journal*, under revision.

Pandita, R. K., Sharma, G. G., Laszlo, A., Hopkins, K. M., Davey, S., Chakhparonian, M., Gupta, A., Wellinger, R. J., Zhang, J., Powell, S. N. et al. (2006). Mammalian Rad9 plays a role in telomere stability, S- and G2-phase-specific cell survival, and homologous recombinational repair. *Mol Cell Biol* **26**, 1850-64.

Parrilla-Castellar, E. R., Arlander, S. J. and Karnitz, L. (2004). Dial 9-1-1 for DNA damage: the Rad9-Hus1-Rad1 (9-1-1) clamp complex. *DNA Repair (Amst)* **3**, 1009-14.

Perry, J. J., Tainer, J. A. and Boddy, M. N. (2008). A SIM-ultaneous role for SUMO and ubiquitin. *Trends Biochem Sci* **33**, 201-8.

Potts, P. R. and Yu, H. (2005). Human MMS21/NSE2 is a SUMO ligase required for DNA repair. *Molecular and Cellular Biology* **25**, 7021-32.

Potts, P. R. and Yu, H. (2007). The SMC5/6 complex maintains telomere length in ALT cancer cells through SUMOylation of telomere-binding proteins. *Nature Structural & Molecular Biology* **14**, 581-90.

Quimby, B. B., Yong-Gonzalez, V., Anan, T., Strunnikov, A. V. and Dasso, M. (2006). The promyelocytic leukemia protein stimulates SUMO conjugation in yeast. *Oncogene* **25**, 2999-3005.

Rothbauer, U., Zolghadr, K., Tillib, S., Nowak, D., Schermelleh, L., Gahl, A., Backmann, N., Conrath, K., Muyldermans, S., Cardoso, M. C. et al. (2006). Targeting and tracing antigens in live cells with fluorescent nanobodies. *Nat Methods* **3**, 887-9.

Saitoh, N., Uchimura, Y., Tachibana, T., Sugahara, S., Saitoh, H. and Nakao, M. (2006). In situ SUMOylation analysis reveals a modulatory role of RanBP2 in the nuclear rim and PML bodies. *Exp Cell Res* **312**, 1418-30.

Shen, T. H., Lin, H. K., Scaglioni, P. P., Yung, T. M. and Pandolfi, P. P. (2006). The mechanisms of PML-nuclear body formation. *Mol Cell* **24**, 331-9.

Song, J., Zhang, Z., Hu, W. and Chen, Y. (2005). Small ubiquitin-like modifier (SUMO) recognition of a SUMO binding motif: a reversal of the bound orientation. *J Biol Chem* **280**, 40122-9.

Soutoglou, E. and Misteli, T. (2008). Activation of the cellular DNA damage response in the absence of DNA lesions. *Science* **320**, 1507-10.

Takahashi, Y., Lallemand-Breitenbach, V., Zhu, J. and de The, H. (2004). PML nuclear bodies and apoptosis. *Oncogene* **23**, 2819-24.

Tarsounas, M. and West, S. C. (2005). Recombination at mammalian telomeres: an alternative mechanism for telomere protection and elongation. *Cell Cycle* **4**, 672-4.

Tumbar, T., Sudlow, G. and Belmont, A. S. (1999). Large-scale chromatin unfolding and remodeling induced by VP16 acidic activation domain. *Journal of Cell Biology* **145**, 1341-1354.

Van Damme, E., Laukens, K., Dang, T. H. and Van Ostade, X. (2010). A manually curated network of the PML nuclear body interactome reveals an important role for PML-NBs in SUMOylation dynamics. *Int J Biol Sci* **6**, 51-67.

Verdun, R. E. and Karlseder, J. (2007). Replication and protection of telomeres. *Nature* **447**, 924-31.

Wachsmuth, M., Caudron-Herger, M. and Rippe, K. (2008). Genome organization: Balancing stability and plasticity. *Biochim Biophys Acta* **1783**, 2061-2079.

Weidtkamp-Peters, S., Lenser, T., Negorev, D., Gerstner, N., Hofmann, T. G., Schwanitz, G., Hoischen, C., Maul, G., Dittrich, P. and Hemmerich, P. (2008). Dynamics of component exchange at PML nuclear bodies. *J Cell Sci* **121**, 2731-43.

West, S. C. (2003). Molecular views of recombination proteins and their control. *Nat Rev Mol Cell Biol* **4**, 435-45.

Wörz, S., Sander, P., Pfannmöller, M., Rieker, R. J., Joos, S., Mechtersheimer, G., Boukamp, P., Lichter, P. and Rohr, K. (2010). 3D Geometry-based quantification of colocalizations in multi-channel 3D microscopy images of human soft tissue tumors. *IEEE Trans. on Medical Imaging* **29**, 1474-1484.

Wu, G., Jiang, X., Lee, W. H. and Chen, P. L. (2003). Assembly of functional ALT-associated promyelocytic leukemia bodies requires Nijmegen Breakage Syndrome 1. *Cancer Res* **63**, 2589-95.

Wu, G., Lee, W. H. and Chen, P. L. (2000). NBS1 and TRF1 colocalize at promyelocytic leukemia bodies during late S/G2 phases in immortalized telomerase-negative cells. Implication of NBS1 in alternative lengthening of telomeres. *J Biol Chem* **275**, 30618-22.

Yeager, T. R., Neumann, A. A., Englezou, A., Huschtscha, L. I., Noble, J. R. and Reddel, R. R. (1999). Telomerase-negative immortalized human cells contain a novel type of promyelocytic leukemia (PML) body. *Cancer Res* **59**, 4175-4179.

Yu, J., Lan, J., Wang, C., Wu, Q., Zhu, Y., Lai, X., Sun, J., Jin, C. and Huang, H. (2009). PML3 interacts with TRF1 and is essential for ALT-associated PML bodies assembly in U2OS cells. *Cancer Lett* **291**, 177-86.

Zhao, X. and Blobel, G. (2005). A SUMO ligase is part of a nuclear multiprotein complex that affects DNA repair and chromosomal organization. *Proceedings of the National Academy of Sciences of the USA* **102**, 4777-82.

Zhu, X. D., Kuster, B., Mann, M., Petrini, J. H. and de Lange, T. (2000). Cell-cycle-regulated association of RAD50/MRE11/NBS1 with TRF2 and human telomeres. *Nat Genet* **25**, 347-52.

Zolghadr, K., Mortusewicz, O., Rothbauer, U., Kleinhans, R., Goehler, H., Wanker, E. E., Cardoso, M. C. and Leonhardt, H. (2008). A fluorescent two-hybrid assay for direct visualization of protein interactions in living cells. *Mol. Cell Proteomics* **7**, 2279-2287.

Figure legends

Figure 1. Experimental approach for studying de novo formed complexes of PML nuclear bodies at the telomeres referred to as APBs.

(A) Schematic representation of the experimental approach. The U2OS cell clone F6B2 employed in this study has three integration sites of the *lac*O arrays adjacent to the telomeres of chromosomes 6q, 11p, and 12q (Jegou et al., 2009). A GFP tagged protein is recruited to *lac*O arrays via a fusion of LacI repressor to a high affinity GFP binding domain (GBP) and a red fluorescent protein domain (GBP-LacI-RFP). Endogenous interaction partners of the GFP labeled protein were identified by subsequent immunostaining and evaluation of the co-localization of the fluorescence signals by confocal laser scanning microscopy (Deng et al., in preparation; Rothbauer et al., 2006; Zolghadr et al., 2008). (B) The F6B2 U2OS cell line was co-transfected with GFP-PML and GBP-LacI expression vectors. Via binding of GBP-LacI to the *lac*O repeat sequences GFP-PML is recruited to these sites. Staining of the telomeric repeats $TTA(G)_3$ with a Cy3 labeled PNA probe revealed the co-localization of telomeres with the GFP-PML signal on the confocal images (see arrows). This indicates the formation of bona fide APBs at the three telomere sites of chromosomes 6q, 11p, and 12q. Scale bar is 10 µm.

Figure 2. Formation of a de novo APB by recruitment of PML and Sp100 protein.

Cells were co-transfected with GBP-LacI-RFP and the indicated GFP constructs. This leads to the tethering of the GFP tagged protein to the three *lac*O labeled telomeres. Association of the main APB components, PML, Sp100, and SUMO, was detected via immunostaining of endogenous proteins and evaluating the co-localization of the two fluorescence signals in optical sections obtained by confocal laser scanning microscopy imaging. Scale bars are 10 µm. (A) Recruitment of GFP-PML yields 100% co-localization with endogenous Sp100 as opposed to 24 ± 5 % in the absence of GFP-PML ($p < 0.0001$). (B) GFP-Sp100 leads to 100% co-localization with endogenous PML versus a control value of 32 ± 5 % in the absence of GFP-Sp100 ($p < 0.0001$). (C, D) GFP-PML induces 93 ± 9 % (endogenous SUMO1) and 98 ± 11 % (endogenous SUMO2/3) co-localization as opposed to 32 ± 5 % and 24 ± 4 % in the control experiments, in which GFP-PML was absent ($p < 0.0001$ for both

analyses). (E) Recruitment of the isolated GFP domain. This leads to a co-localization of only 19 ± 5 % with endogenous PML, which does not significantly differ from the 20-30 % background observed in the control transfection with only GBP-LacI-RFP (p = 0.48).

Figure 3. Initiation of APB formation by recruitment of the SUMO domain.

After co-transfection of GBP-LacI-RFP and GFP- or YFP-SUMO constructs, cells were subjected to immunostaining for endogenous PML protein in order to detect APB formation on CLSM images from the degree of co-localization of PML signals and the GFP/YFP-SUMO label at the three telomeres. The co-localization background signal was 19 ± 5 % measured by transfections with GBP-LacI-RFP and the isolated GFP domain. Scale bars are 10 µm. (A) GFP-SUMO1, 82 ± 10 % co-localization (p < 0.0001). (B) GFP-SUMO2, 80 ± 10 % co-localization (p < 0.0001). (C) GFP-SUMO3, 85 ± 10 % co-localization (p < 0.0001). (D) Non-conjugable YFP-SUMO1ΔC7, 77 ± 6 % co-localization (p < 0.0001). (E) Non-conjugable GFP-SUMO2ΔC4, 46 ± 5 % co-localization (p < 0.0001). (F) Non-conjugable GFP-SUMO3ΔC13, 45 ± 7 % co-localization (p < 0.0005). (G) Non-conjugable and not SIM-interacting YFP-SUMO1ΔC7(-) with amino acid exchanges V38A/K39A that prevent the recognition by SIMs, 27 ± 4 % co-localization (p = 0.16). (H) Non-conjugable C-terminal tagged SUMO3-GFP (see also Fig. S3), 30 ± 4 % co-localization (p = 0.07).

Figure 4. Initiation of APB formation by shelterin and DNA repair/recombination proteins.

Confocal images of cells that were co-transfected with GBP-LacI-RFP (column 1), the indicated GFP fusion protein (column 2, merge of RFP and GFP signal in column 3), and immunostained for endogenous PML protein to determine APB formation (column 4). The co-localization of the GFP signal at telomeric *lac*O arrays with the immunofluorescence of endogenous PML at these sites (column 5) yielded 19 ± 5 % in the control, in which an isolated GFP domain was recruited. Scale bars are 10 µm. The propensity of proteins to induce APB formation when recruited to the telomeres as GFP fusions was evaluated in terms of co-localization with endogenous PML. This yielded values of (A) GFP-TRF1: 70 ± 8 % (p < 0.0001). (B) GFP-TRF2: 85 ± 7 % (p < 0.0001). (C) NBS1-GFP: 83 ± 9 % (p <

0.0001). (D) Rad51-GFP: 40 ± 4 % (p < 0.0005). (E) GFP-Rad9: 59 ± 6 % (p < 0.0001). (F) GFP-Rad17: 31 ± 6 % (p = 0.10).

Figure 5. Detection of endogenous proteins that are bona fide components of functional APBs.

Confocal images of F6B2 cells transfected with GBP-LacI-RFP (column 1) and GFP-PML (column 2, merge of RFP and GFP signal in column 3) to induce APB formation, and then immunostained to detect interacting endogenous DNA repair/recombination factors (column 4) from co-localization of the GFP-PML and the immunofluorescence signal (column 5). Controls were transfected with GBP-LacI-RFP only or with GBP-LacI-RFP and GFP. In order to compare the composition of non-telomeric de novo PML-NBs the same experiments were conducted with the U2OS cell clone F42B8, which has a pericentric *lac*O integration. Scale bars are 10 µm. (A) Co-localization with endogenous NBS1 increased from 12 ± 3 to 21 ± 4 % at telomeres (p < 0.05) and from 18 ± 5 to 60 ± 9 % at pericentromeres (p < 0.0001). (B) Co-localization with endogenous Rad9 increased from 17 ± 4 to 69 ± 8 % at telomeres and from 23 ± 5 to 88 ± 11 % at pericentromeres (p < 0.0001 for both analyses). (C) Co-localization with endogenous Rad17 increased from 17 ± 3 to 36 ± 6 % at telomeres and from 28 ± 6 to 56 ± 8 % at pericentromeres (p < 0.0005 for both analyses).

Figure 6. MMS21 induced de novo APB assembly.

Cells were co-transfected with GBP-LacI-RFP or GBP-LacI and GFP fusions of either PML or the SUMO E3 ligase MMS21. Subsequently, samples were stained with the indicated antibodies. Scale bars are 10 µm. (A) Nuclear body formation was induced by recruitment of GFP-PML to telomeric *lac*O arrays. The presence of endogenous MMS21 was evaluated by immunofluorescence after recruitment of GFP-PML and increased from 16 ± 5 % to 68 ± 7 % (p < 0.0001). (B) Same as panel A but the pericentric locus was studied. Endogenous MMS21 co-localization values were 79 ± 9 % after GFP-PML recruitment as opposed to 28 ± 5 % in the GFP control (p < 0.0001). (C) Recruitment of GFP-MMS21 with GBP-LacI-RFP to the *lac*O labeled telomeres induced 86 ± 9 % co-localization with endogenous PML protein (p < 0.0001). (D) GFP-MMS21 was tethered to the *lac*O arrays via co-transfection with the GBP-LacI construct. Co-localizations of endogenous PML and Rad9 proteins with

the GFP-MMS21 bound *lac*O arrays were detected via immunofluorescence. The majority of *lac*O tagged telomeres showed a co-localization with endogenous PML after GFP-MMS21 recruitment (indicated by arrows in D1, magnification in D2), whereas endogenous Rad9 was found only at a fraction of these sites (filled arrows in D1, magnification in D3). Scale bars are 10 µm in D1 and 0.5 µm in D2 and D3. (E) Quantification of PML/Rad9 co-localization after GFP-MMS21 tethering (n = 182 *lac*O tagged telomeres). Analysis of endogenous APBs that were identified via transfection of GFP-TRF2 in U2OS cells revealed that 16 ± 1 % of telomeres co-localized with PML and 15 ± 1% with Rad9. A percentage of 2.0 ± 0.3 % of telomeres were associated with only PML, and 0.9 ± 0.2 % with only Rad9 (n = 1722 telomeres). Note the different scale of the y-axis.

Figure 7. Induction of DNA repair synthesis by de novo formed APBs.

APB formation was initiated by recruiting GFP-PML to the three *lac*O labeled telomeres in F6B2 cells and then analyzed in terms of activities associated with DNA double-strand break repair and DNA synthesis at these sites. The same experiments were performed using F42B8 cells containing a pericentric *lac*O insertion. Scale bars are 10 µm. (A) The co-localization of APBs with the phosphorylated histone variant γH2A.X increased from 20 ± 4 without GFP-PML transfection to 31 ± 6 %, indicative of an induction of double-strand break repair processes ($p < 0.05$). In contrast to that, there was no significant difference in F42B8 cells regarding the percentage of γH2A.X positive *lac*O arrays with or without GFP-PML recruitment (14 ± 4 % when GFP was recruited and 16 ± 4 % after GFP-PML recruitment, $p = 0.55$). (B) An increase in non-replicative DNA synthesis as detected by BrdU incorporation was found with an 18 ± 4 % fraction of APBs as compared to 7 ± 3 % in the control when only GBP-LacI-RFP was transfected ($p < 0.05$). Recruiting GFP-PML to a pericentric site did not induce a significant change in the portion of these sites co-localizing with the BrdU signal (4 ± 2 % with only GFP and 8 ± 3 % with GFP-PML recruited, $p = 0.38$).

Figure 8. Induction of telomere repeat extension by de novo formed APBs.

Changes in the length of the telomere repeat sequence $TTA(G)_3$ upon de novo APBs assembly were evaluated in FISH experiments with a Cy3 labeled PNA probe complementary to this sequence. In the control, GBP-LacI was co-transfected with the

isolated GFP domain instead of GFP-PML. (A) Four examples (numbers 1-4) for the evaluation of the telomere repeat length at the *lac*O tagged telomeres are depicted. The normalized telomere length was determined as the intensity ratio of the TTA$(G)_3$-Cy3 fluorescence intensity at a telomere co-localizing with the *lac*O bound GFP(-PML) label to that of the total Cy3 signal in a given nucleus. A normalized telomere repeat signal of < 0.025 % (equivalent to two times the Cy3 background signal) as in telomere (1) was considered a non-detectable telomere signal. In contrast, the other three telomeres had values of 0.5 % (2), 1.4 % (3) and 3.7 % (4). Scale bars are 0.5 µm. (B) The fraction of detectable telomeric repeats was determined 12, 24, 48, and 96 h after transfection of the telomeric *lac*O containing F6B2 cells and revealed an increase after GFP-PML recruitment as opposed to the GFP only control. The stars refer to values of $p < 0.01$ (*) or $p < 0.0001$ (**). This was not observed when recruiting GFP-PML to pericentric sites in F42B8 cells as determined 24 h after transfection (control: 22 ± 4 %, GFP-PML recruited: 27 ± 5 %, $p = 0.43$). (C) The resulting distribution of detectable telomere (i. e. ≥ 0.025 % telomere repeat signal) was fitted to a one- or two-component Gauss distribution. A ~20 % fraction of telomeres with an increased normalized repeat length of 3.4 ± 0.8 % appeared when APB formation was induced via recruitment of GFP-PML.

Figure 9. Model for the mechanism of APB assembly and telomere elongation.

As described in the text, APB formation can be initiated by the recruitment of the isolated SUMO1 domain or the SUMO E3 ligase MMS21 as well as the telomeric proteins TRF1 and TRF2. Accordingly, we propose that the assembly of an APB is initiated by sumoylation of telomeric proteins. The initial nucleation event triggers a feedback mechanism that leads to the enrichment of PML and Sp100. Additional auto-sumoylated MMS21 is recruited via the SIMs of PML and Sp100 so that the SUMO1 dense region is amplified and propagates to comprise the complete telomere repeat sequence. Our data also suggest that NBS1 is one of the initiating factors for APB formation. Once the structural components of the APB are fully assembled, other proteins like the DNA recombination and repair factors Rad51, Rad9 and Rad17 are recruited to this binding platform. This results in the formation of an APB complex that is functional in telomere extension in a DNA repair process that involves non-replicative

DNA synthesis as shown here by the phosphorylation of H2A.X, the incorporation of BrdU, and the increase of telomeric DNA.

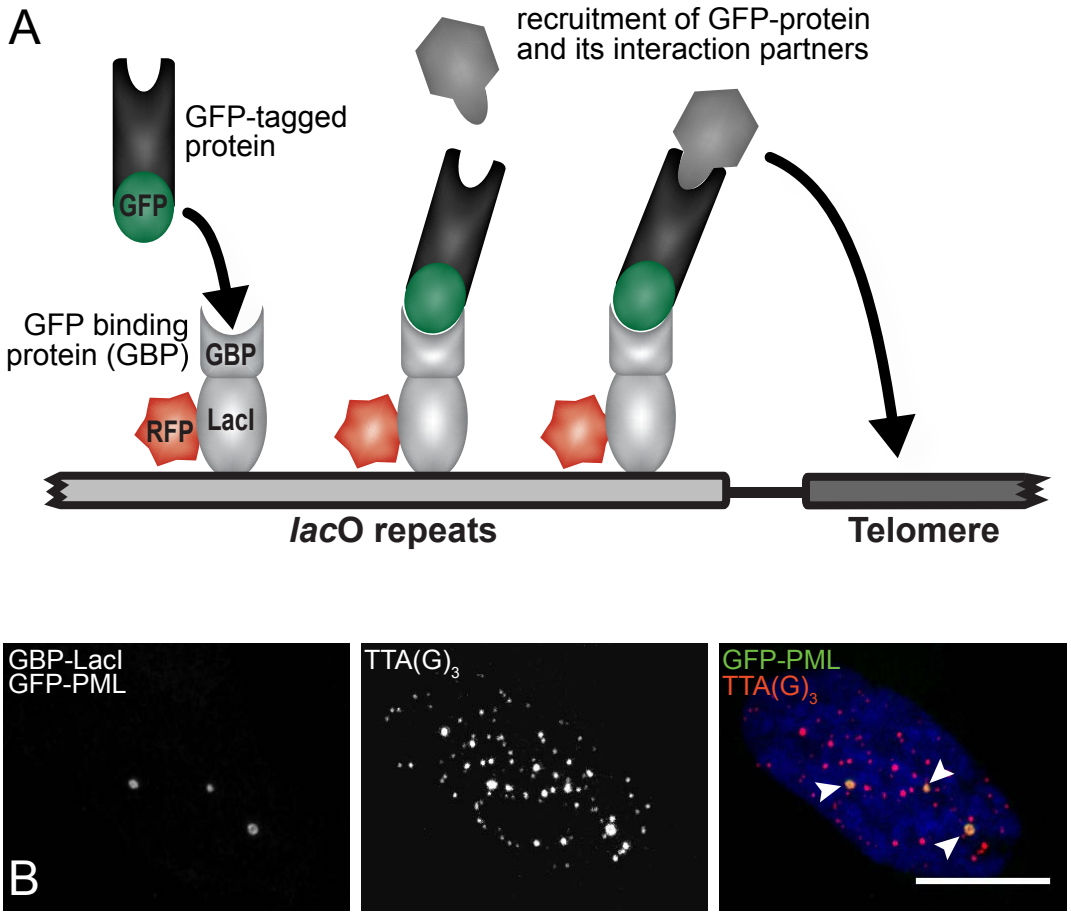

Chung et al, Fig. 1

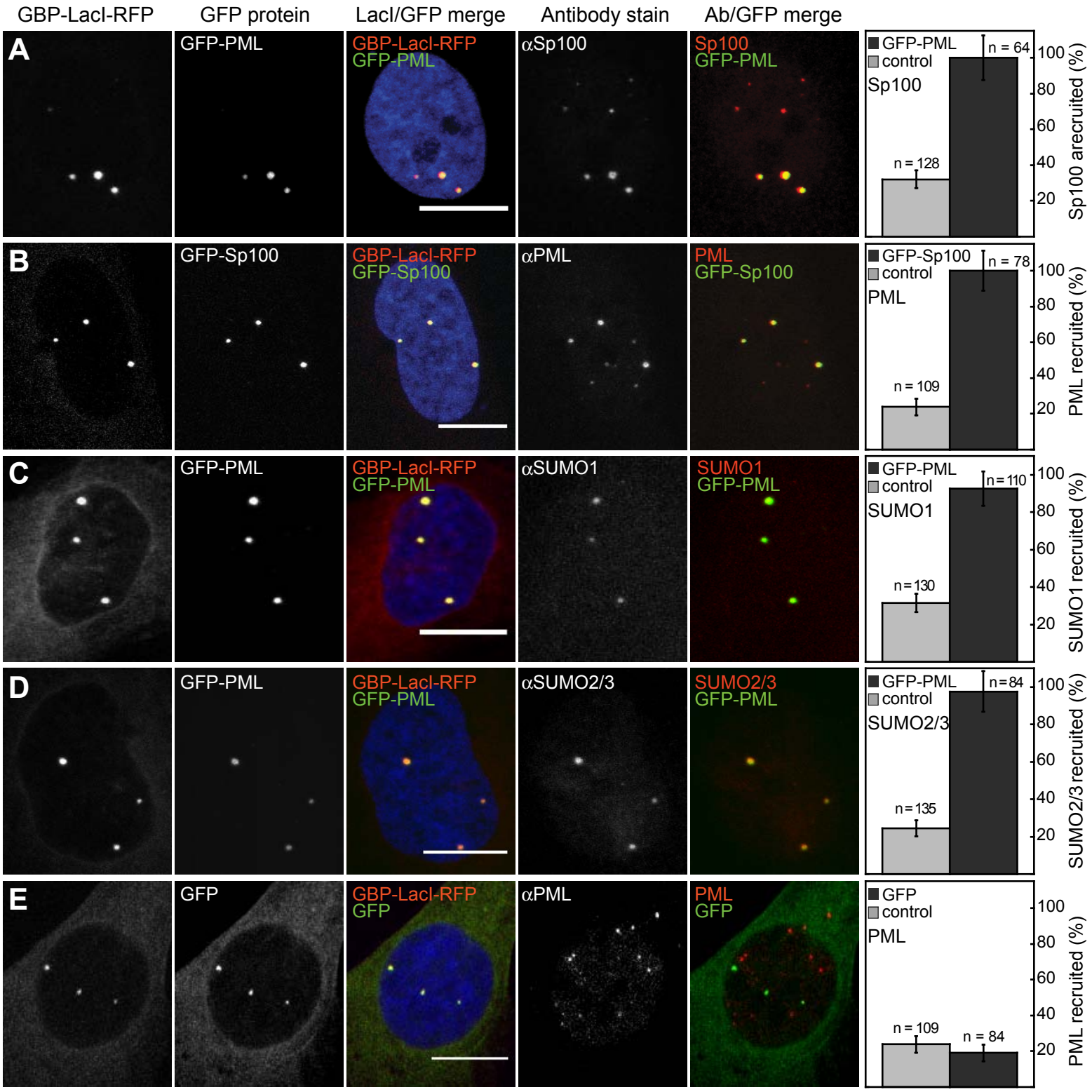

Chung et al, Fig. 2

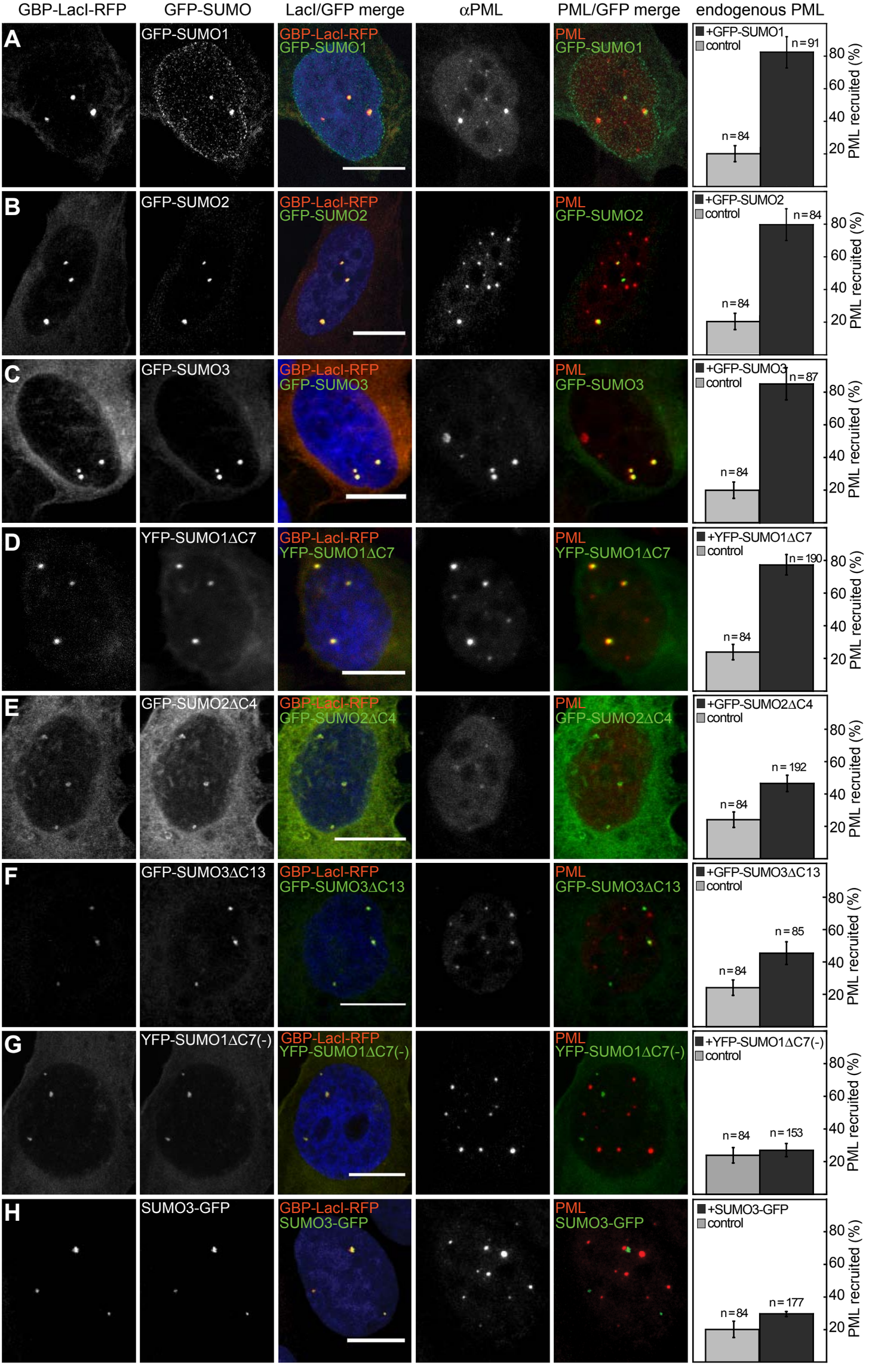

Chung et al, Fig.3

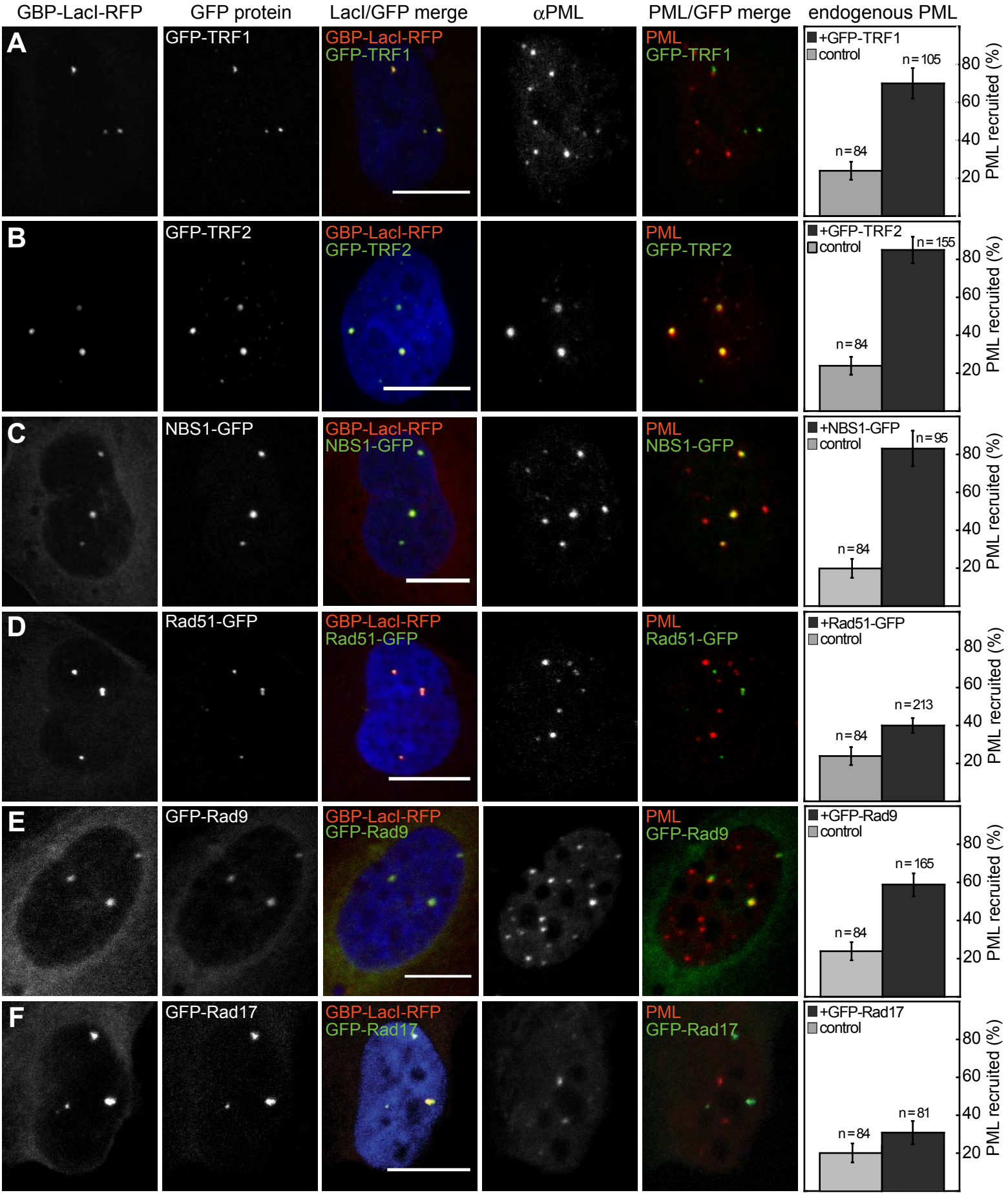

Chung et al, Fig. 4

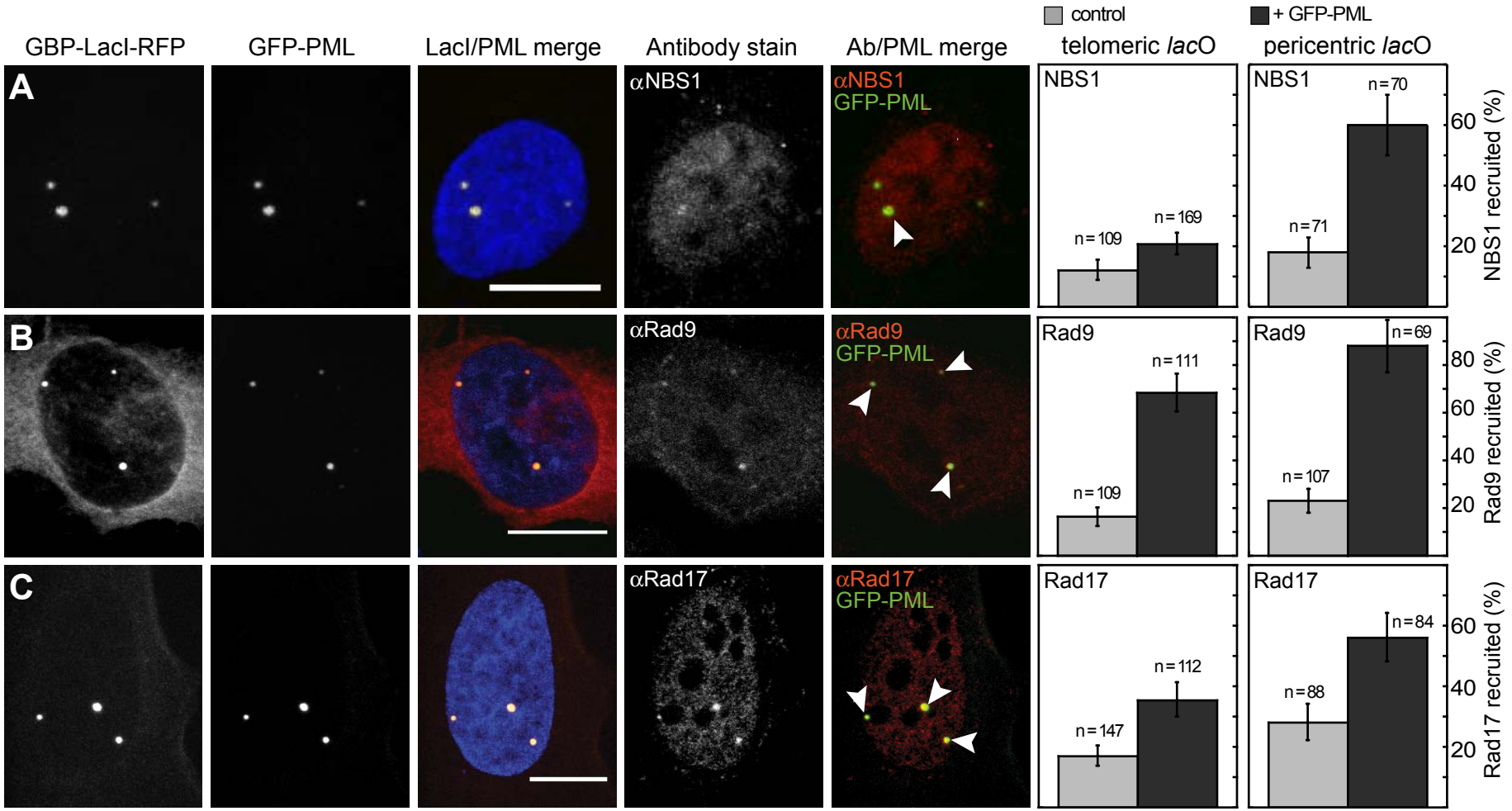

Chung et al, Fig. 5

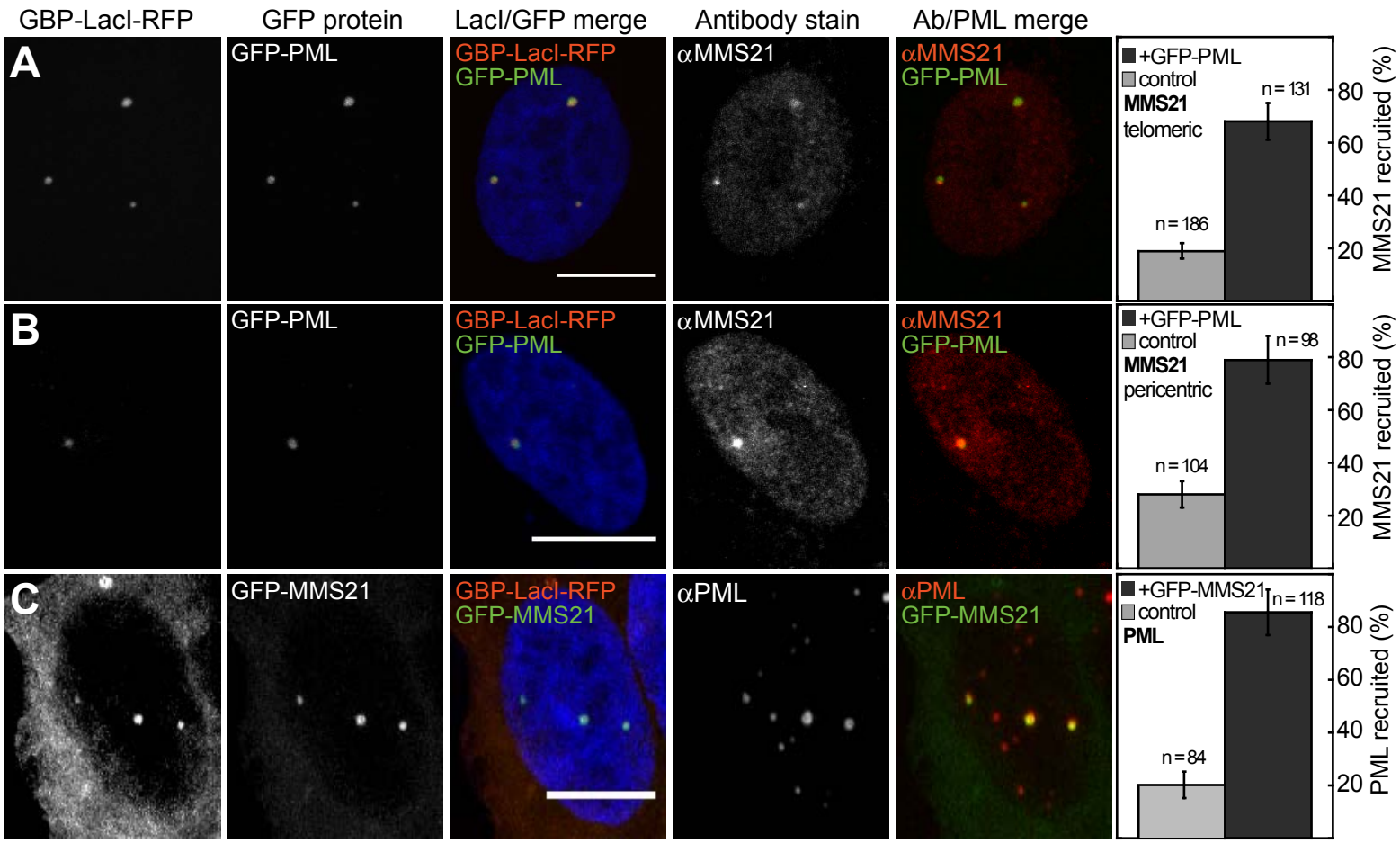

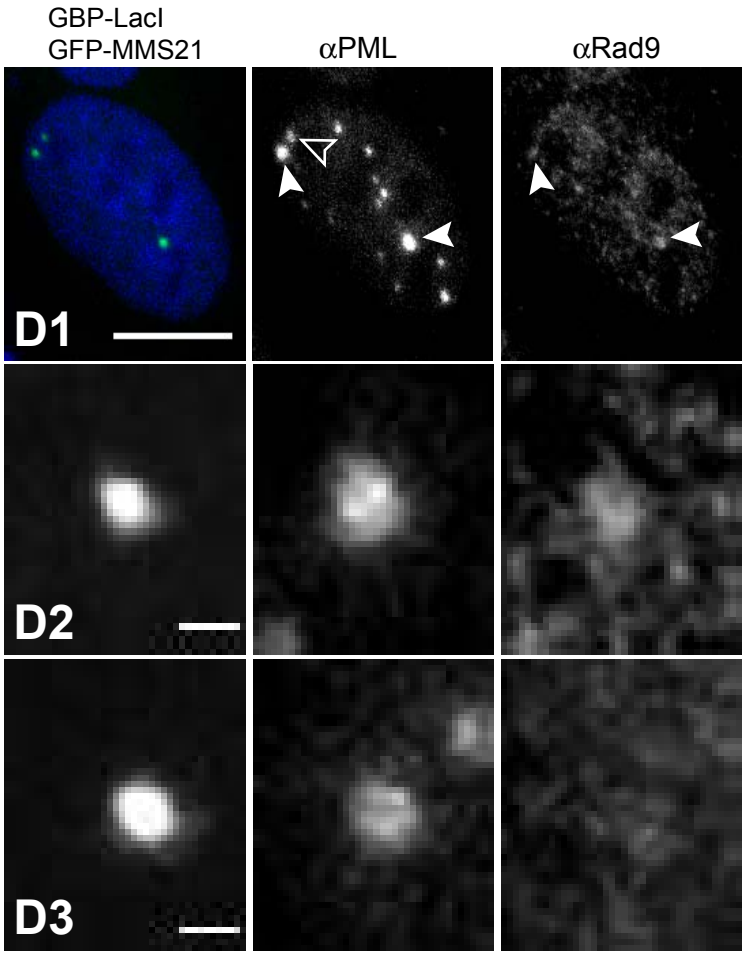

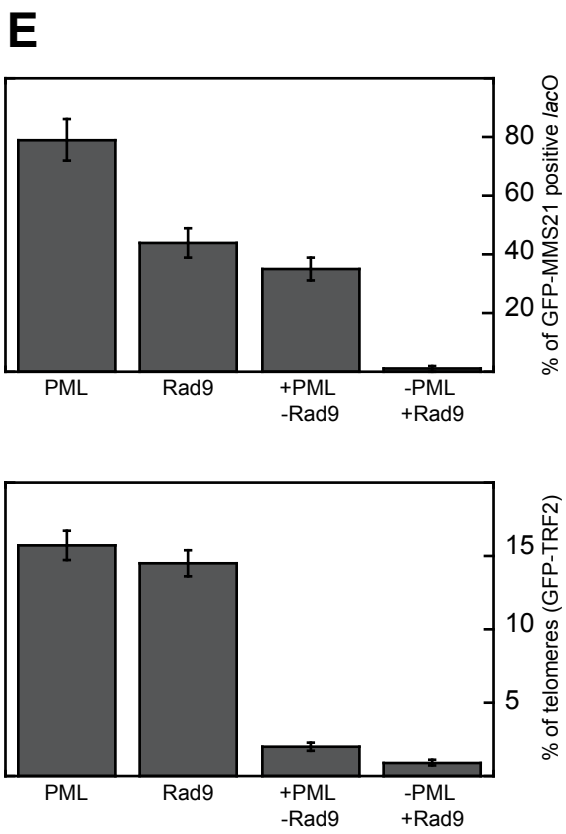

Chung et al, Fig. 6

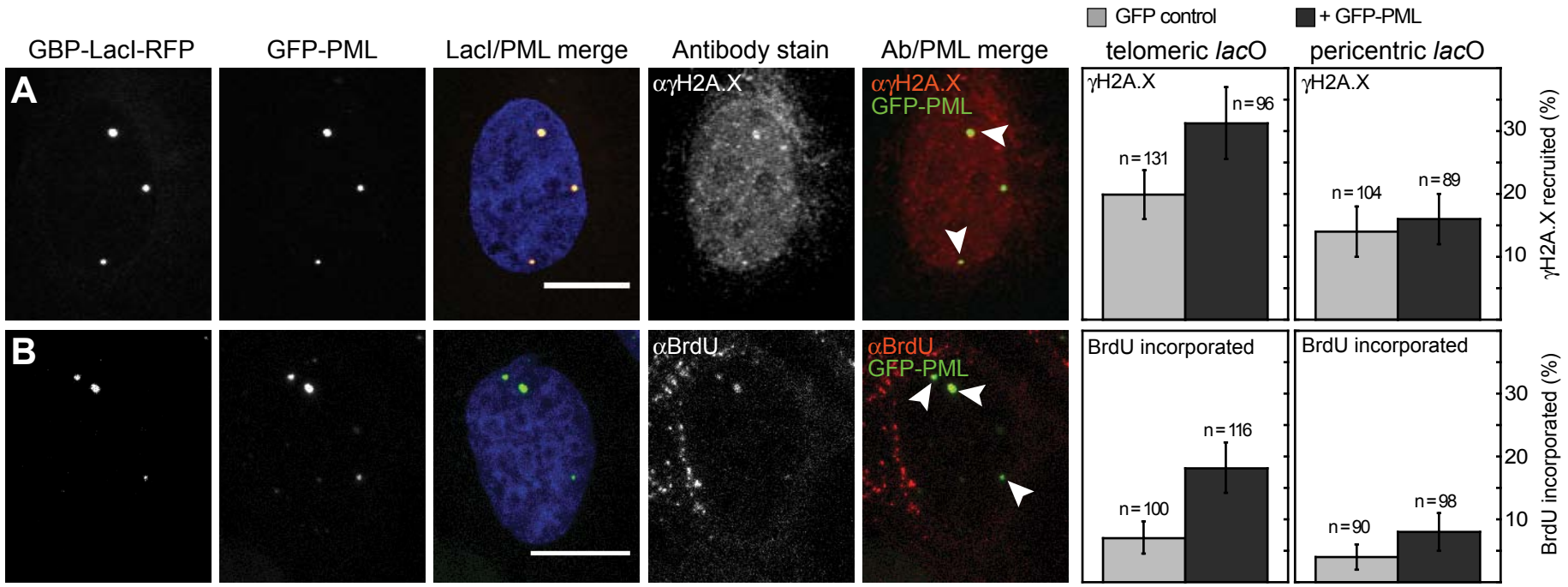

Chung et al, Fig. 7

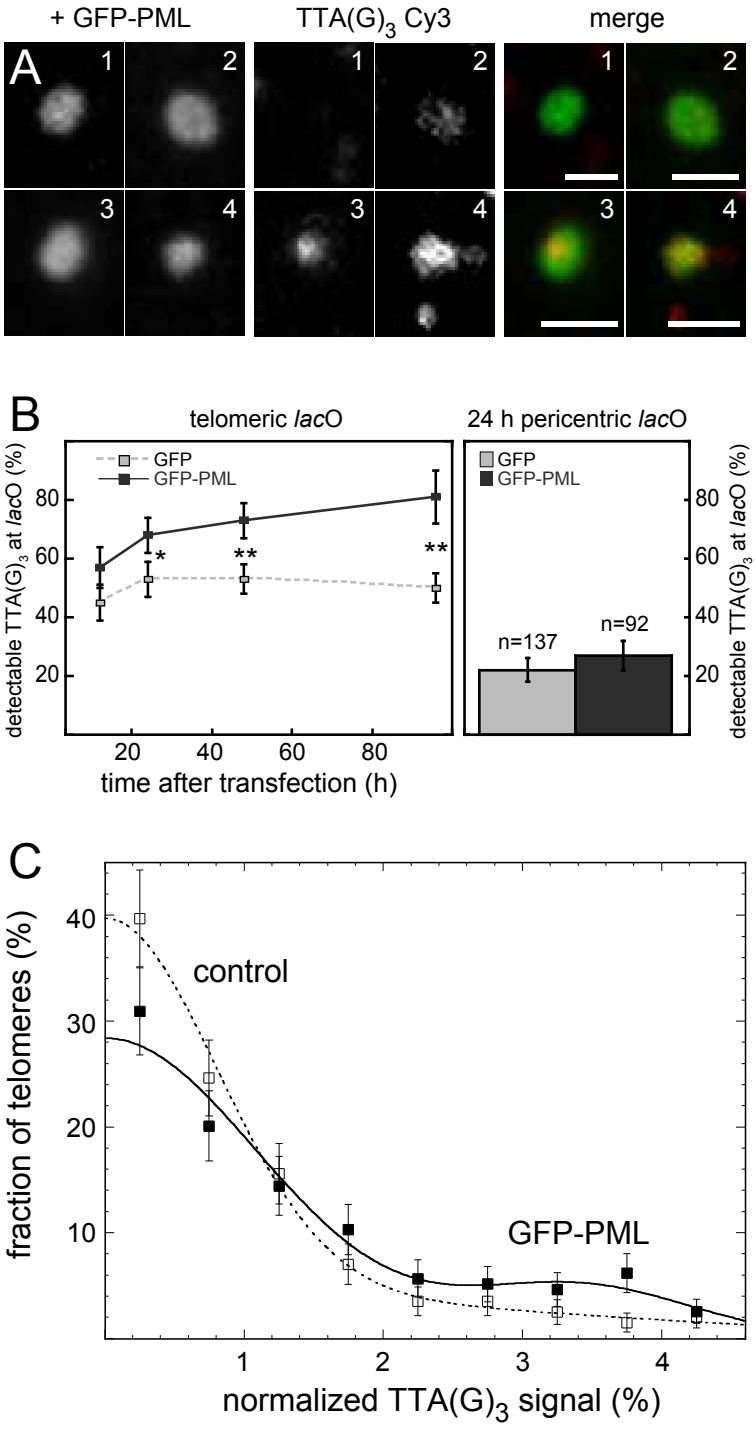

Chung et al, Fig. 8

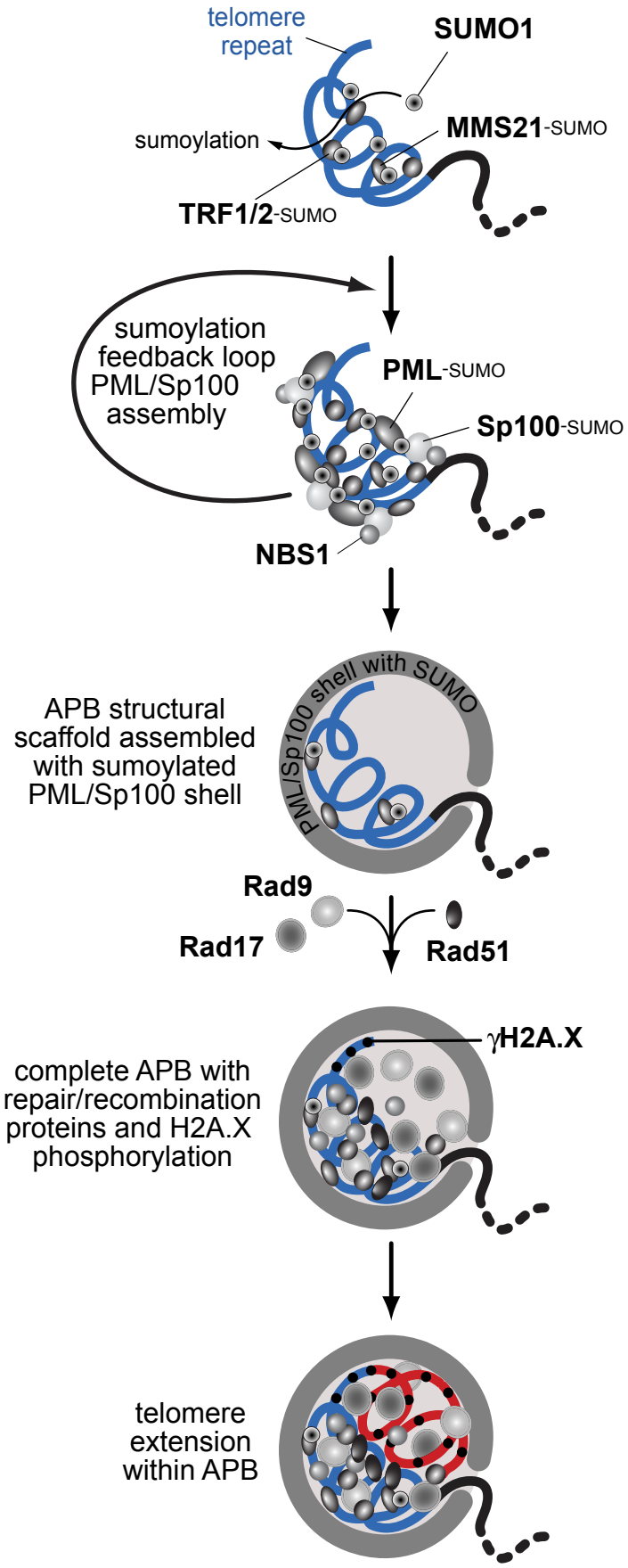

Chung et al, Fig. 9

Table I. APB de novo assembly and recruitment of endogenous proteins

	***lac*O at telomeres 11p, 6q, 12q (F6B2)**		**pericentric *lac*O at 2p (F42B8)**	
Protein	Initiation of APB formation by GFP fusion protein [a]	Recruitment of endogenous protein to de novo APBs [b]	Initiation of APB-like structure assembly by GFP fusion protein [a]	Recruitment of endogenous protein to APB-like compartment [b]
PML	+++	+++	+++	n.d.
Sp100	+++	+++	n.d.	n.d.
SUMO1 wt	+++	+++	n.d.	+++
SUMO2 wt	+++	+++ [c]	n.d.	+++ [c]
SUMO3 wt	+++	+++ [c]	n.d.	+++ [c]
SUMO1ΔC7	++	n.d.	n.d.	n.d.
SUMO2ΔC4	+	n.d.	n.d.	n.d.
SUMO3ΔC13	+	n.d.	n.d.	n.d.
SUMO3-GFP	-	n.d.	n.d.	n.d.
SUMO1ΔC7(-)	-	n.d.	n.d.	n.d.
TRF1	++	n.d.	++	n.d.
TRF2	+++	n.d.	++	n.d.
MMS21	+++	++	+++	++
NBS1	+++	+	+++	++
Rad51	+	n.d.	-	n.d.
Rad9	++	++	n.d.	+++
Rad17	-	+	n.d.	++
γH2A.X	n.d.	+	n.d.	-
GFP	-	n.d.	-	n.d.

The measured degree of co-localization at the *lac*O loci was: +++, > 80 %; ++, > 50 %; +, > 20 %; - , no significant enrichment over background ($p > 0.05$); n.d., not determined.

[a] The indicated GFP fusion proteins were bound to the lacO arrays via GBP-LacI-RFP. APB formation was evaluated by immunostaining for endogenous PML at these sites except for PML where endogenous Sp100 was measured.

[b] The de novo APB formation was induced by tethering GFP-PML (except for PML when GFP-Sp100 was used). Recruitment of endogenous proteins co-localizing with the GBP-LacI-RFP signal was detected by immunofluorescence.

[c] One single antibody was used for detecting both endogenous isoforms SUMO2 and SUMO3 simultaneously.

Supplemental material

I. Chung, H. Leonhardt & K. Rippe, De novo assembly of a PML nuclear subcompartment occurs via multiple pathways and induces telomere elongation

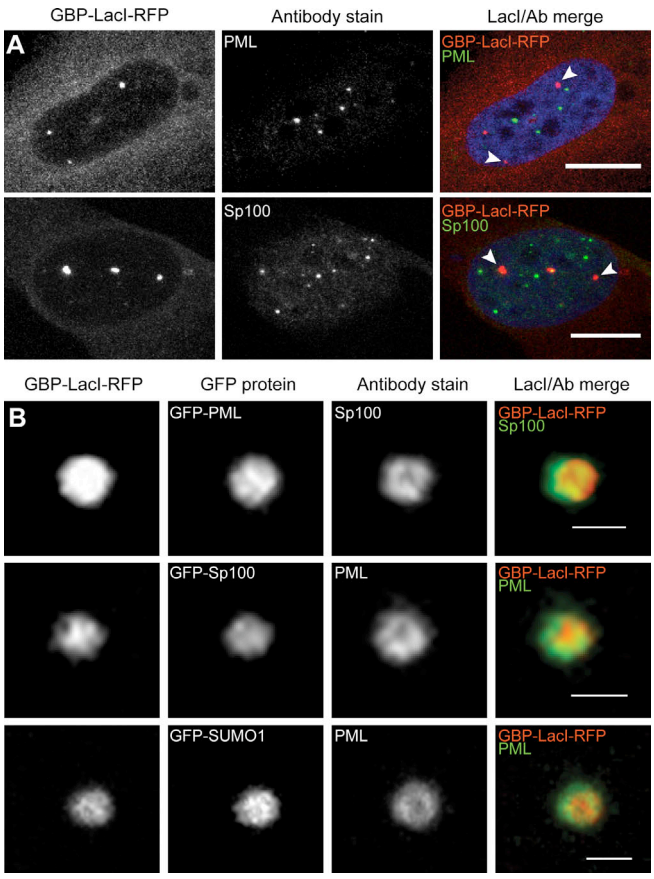

Figure S1. Characterization of de novo APBs.

(A) GBP-LacI-RFP alone does not induce APB formation. CLSM images of cells transfected only with GBP-LacI-RFP. Only the background level of co-localization of the *lac*O arrays with the PML-NB marker proteins PML and Sp100 was observed, yielding 24 ± 5 % for PML and 32 ± 5 % for Sp100 (see histograms in Fig. 2). Arrows indicate *lac*O labeled telomeres without accumulation of PML-NB components. Scale bars are 10 µm. Cells were immunostained for endogenous PML and Sp100 as indicated. (B) CLSM images of APBs formed de novo by recruitment of GFP-PML, GFP-Sp100 or GFP-SUMO1. Endogenous PML-NB components Sp100 or PML were visualized at the *lacO* arrays after co-transfection of GBP-LacI-RFP with the different GFP constructs. The structure of the de novo formed APBs was indistinguishable from that reported previously for endogenous APBs at the resolution of a conventional CLSM (Jegou et al., 2009; Lang et al., 2010). Scale bars are 1 µm.

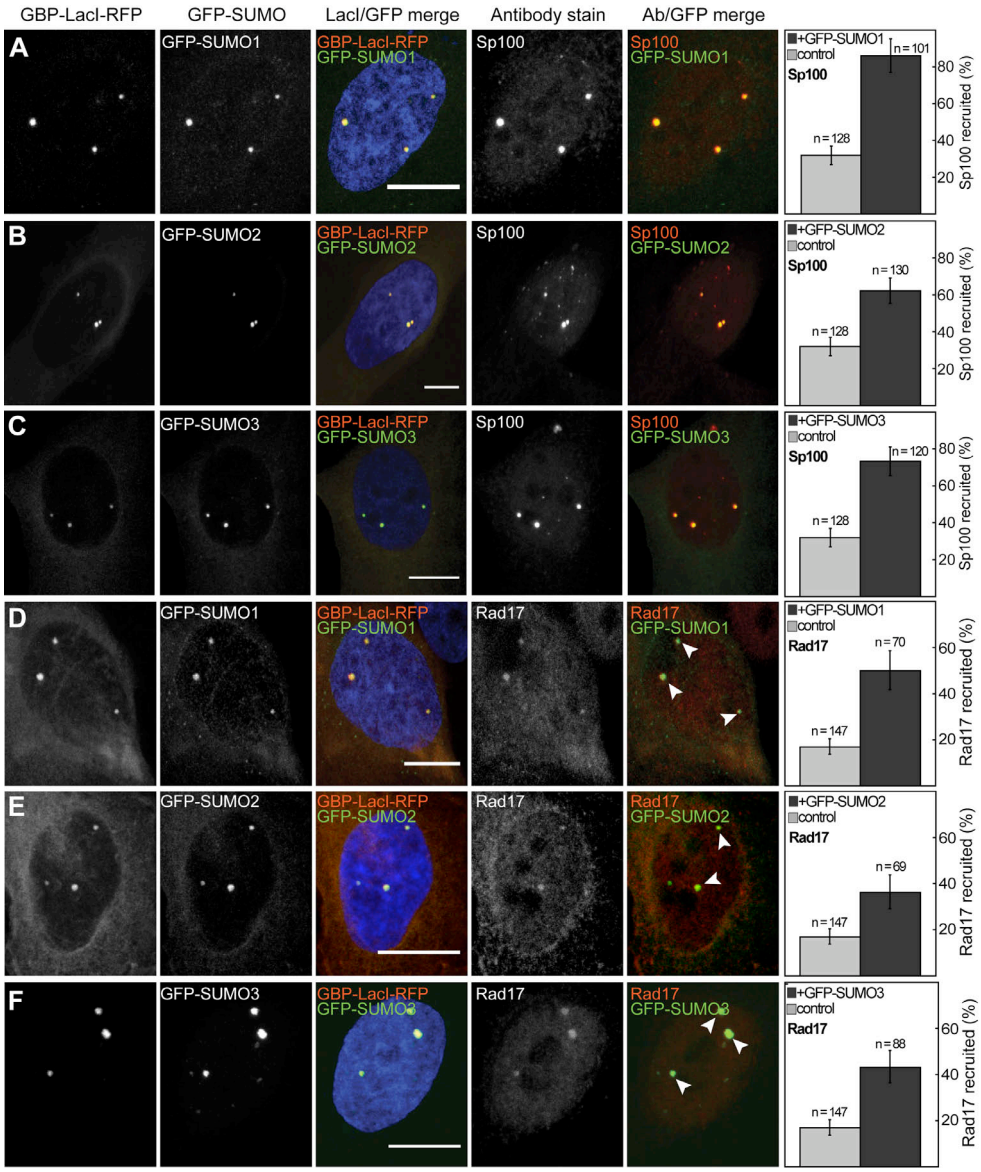

Figure S2. Recruitment of Sp100 and Rad17 by tethering SUMO1/2/3 to the *lac*O arrays.
Cells were co-transfected with GBP-LacI-RFP and the indicated GFP-SUMO constructs. The presence of endogenous Sp100 (A-C) or Rad17 (D-F) was detected by immunostaining and co-localization was determined on CLSM images. Scale bars are 10 µm. The co-localization background signal in transfections with only GBP-LacI-RFP was 32 ± 5 % (Sp100) or 17 ± 3 % (Rad17). (A) GFP-SUMO1 and endogenous Sp100, 86 ± 9 % co-localization ($p < 0.0001$). (B) GFP-SUMO2 and endogenous Sp100, 62 ± 7 % co-localization ($p < 0.0001$). (C) GFP-SUMO3 and endogenous Sp100, 73 ± 8 % co-localization ($p < 0.0001$). (D) GFP-SUMO1, 50 ± 9 % co-localization with endogenous Rad17 ($p < 0.0001$). (E) GFP-SUMO2, 36 ± 7 % co-localization with endogenous Rad17 ($p < 0.005$). (F) GFP-SUMO3 43 ± 7 % co-localization with endogenous Rad17 ($p < 0.0001$).

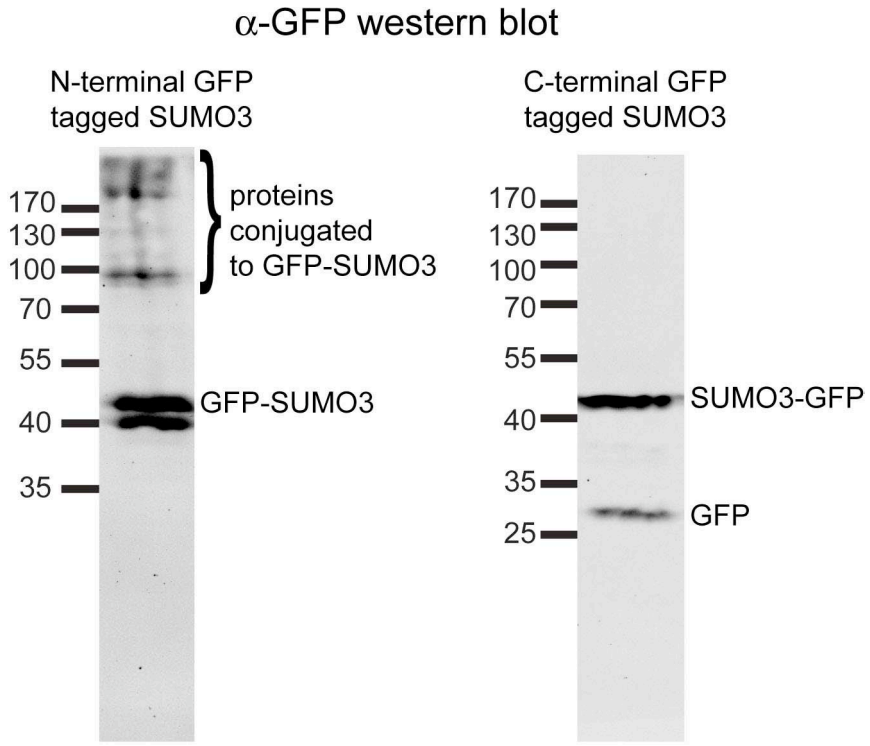

Figure S3. N-terminal GFP tagged but not C-terminal GFP tagged SUMO can be conjugated to target proteins.

Cells were transfected with GFP-SUMO3 or SUMO3-GFP, and whole cell lysates were subjected to western blot analysis using an α-GFP antibody. After transfection of cells with N-terminal tagged GFP-SUMO3 high molecular weight bands were detected demonstrating the presence of proteins that have GFP-SUMO3 covalently bound. For SUMO3-GFP with a C-terminal GFP fusion, only SUMO3-GFP and some free GFP were detected with the α-GFP antibody. This result can be explained by the mechanism of the sumoylation reaction, during which C-terminal amino acids are cleaved from the SUMO precursor. This exposes a glycine residue that subsequently can be attached to a lysine of the target protein. Only a small fraction of the transfected SUMO-GFP is processed, so that residual amounts of free GFP are detected whereas the large majority remains as uncleaved SUMO3-GFP. It is noted that conjugation of SUMO3 from the SUMO3-GFP substrate would not be detected after cleavage of the GFP domain with the a-GFP antibody.

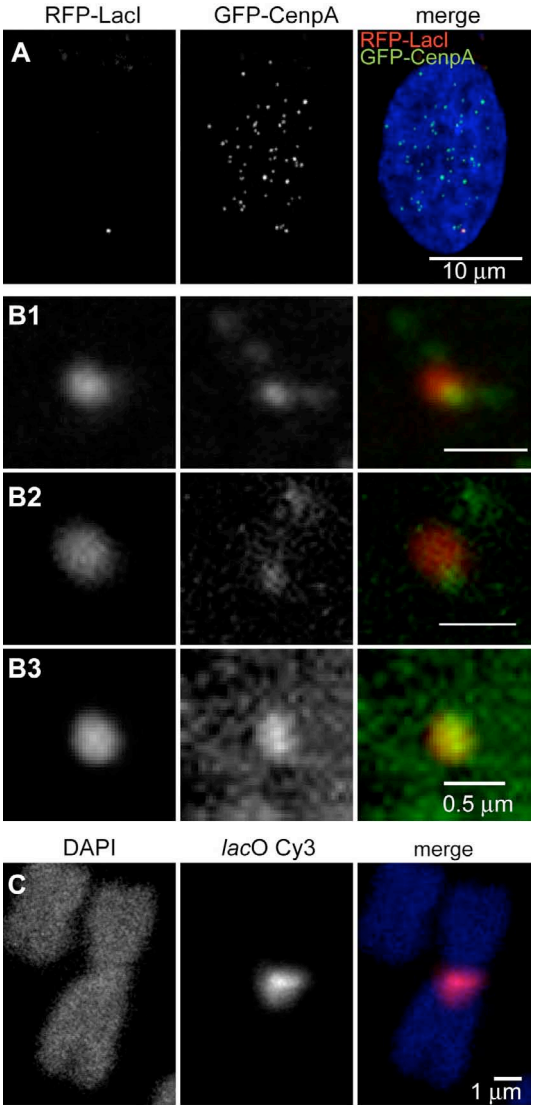

Figure S4. F42B8 cells have a *lac*O array integrated at a pericentric region.

Cells were co-transfected with RFP-LacI and the centromeric protein GFP-CenpA (A, B). CLSM images reveal an overlap of the RFP-LacI signal with the centromeric marker CenpA (A), which was confirmed by examination of higher magnifications of the spots (B1-3). (C) Additionally, metaphase chromosomes of the F42B8 cell clone were prepared, and FISH was conducted using a Cy3 labeled oligonucleotide probe against the *lac*O sequence indicating the site of integration next to the centromere.

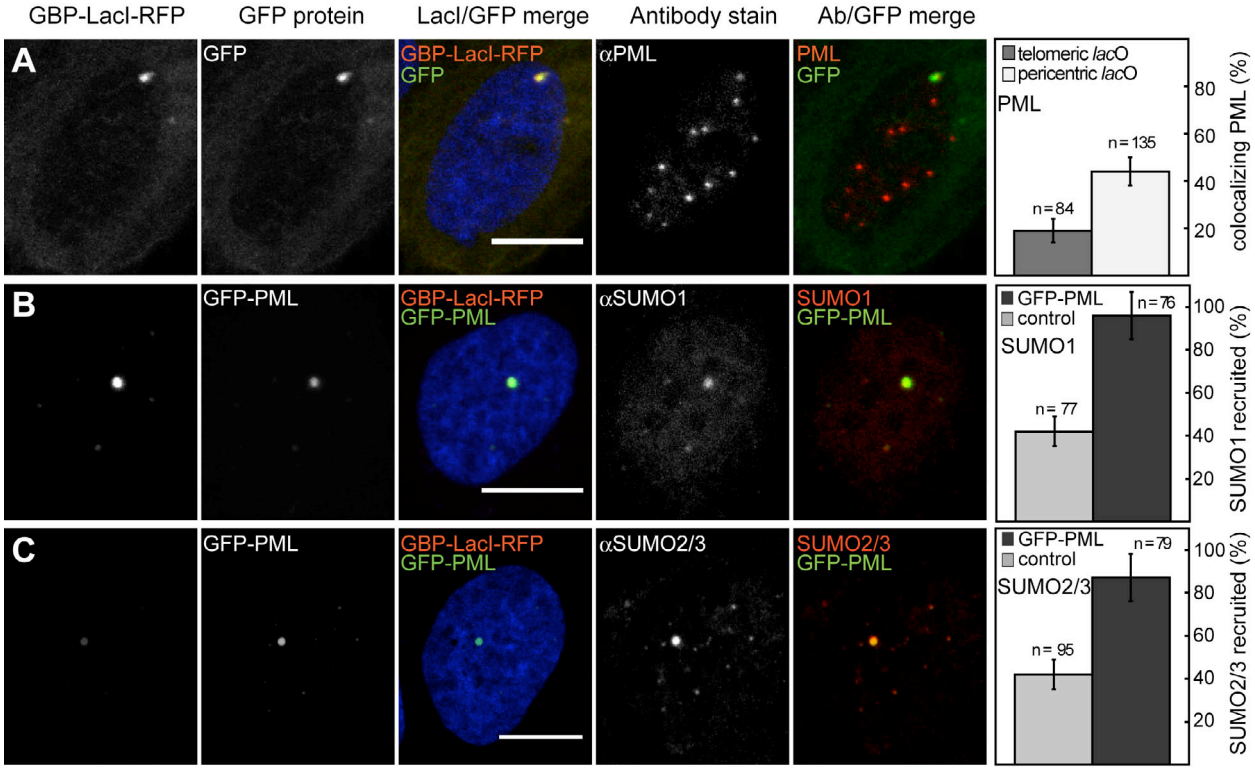

Figure S5. De novo PML-NBs assemble at a pericentric *lac*O array.

F42B8 cells were co-transfected with GBP-LacI-RFP and GFP or GFP-PML, and the presence of endogenous PML was detected by immunofluorescence. (A) Pericentric *lac*O arrays co-localize to a higher extend with endogenous PML (44 ± 6 %) as compared to the telomeric *lac*O arrays (19 ± 5 %), $p < 0.0005$. (B) Recruitment of GFP-PML induces the enrichment of endogenous SUMO1 from 42 ± 7 % in the control, when only GFP was recruited, to 96 ± 11 % ($p < 0.0001$). (C) Recruitment of GFP-PML induces the enrichment of endogenous SUMO2/3 from 42 ± 7 % in the control to 87 ± 11 % ($p < 0.0001$).

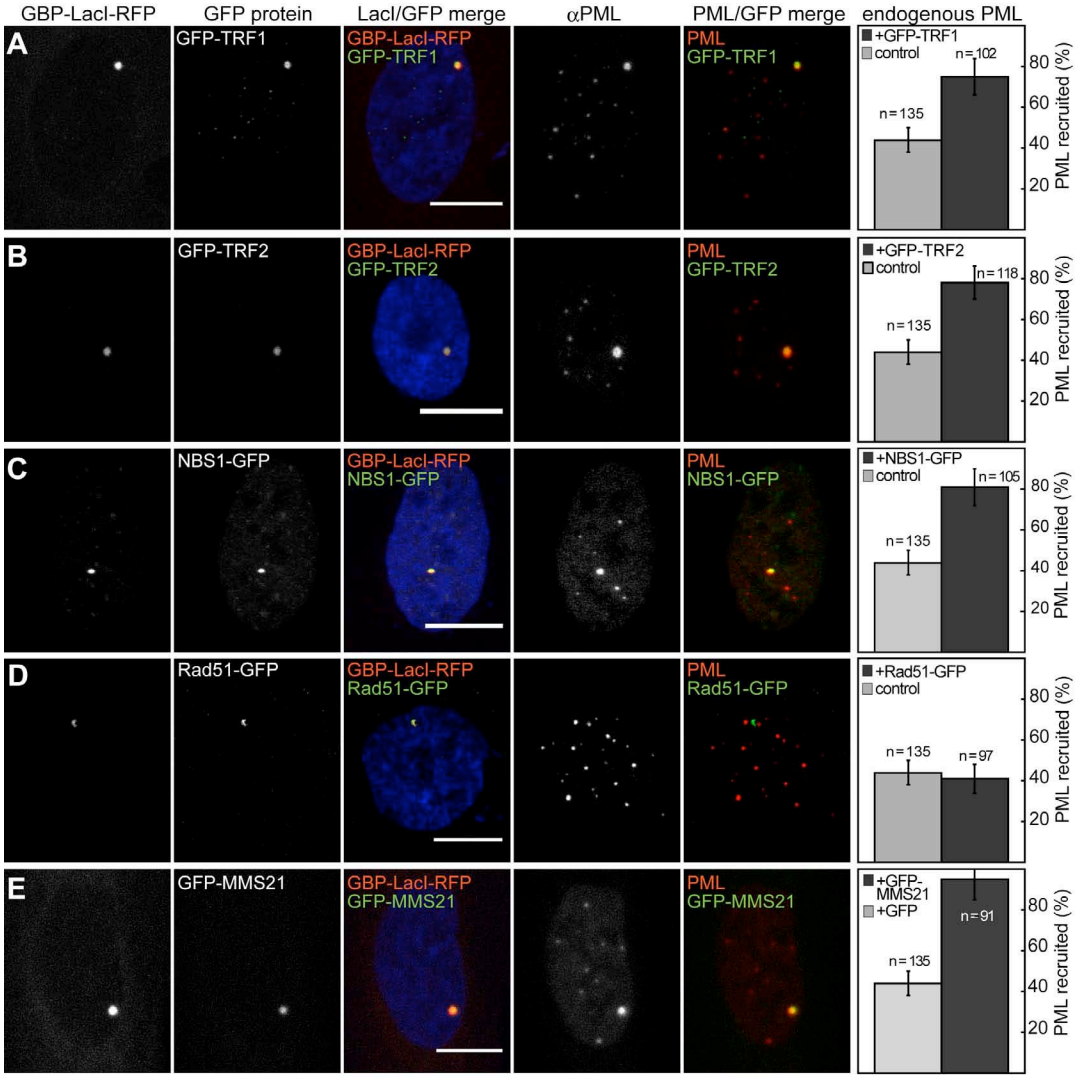

Figure S6. Recruitment of several GFP tagged proteins to a pericentric *lac*O array.

F42B8 cells were co-transfected with GBP-LacI-RFP and the indicated GFP-constructs and subsequently stained for endogenous PML. The co-localization background signal was 44 ± 5 % measured by transfections with GBP-LacI-RFP and the isolated GFP domain. Scale bars are 10 µm. (A) Recruitment of the shelterin factor GFP-TRF1 increased the presence of endogenous PML to 75 ± 9 % ($p < 0.0001$). (B) Another shelterin component, GFP-TRF2, led to an increase in co-localization with endogenous PML to 78 ± 8 % ($p < 0.0001$). (C) After recruitment of NBS1-GFP the fraction of PML positive *lac*O arrays increases to 81 ± 9 % ($p < 0.0001$). (D) The recombination factor Rad51-GFP was not able to induce accumulation of endogenous PML at the pericentric lacO array as only 41 ± 7 % of co-localization was detected ($p = 0.69$). (E) Recruitment of the SUMO E3 ligase GFP-MMS21 increases the presence of endogenous PML at the pericentric *lac*O insertion from 44 ± 6 % to 95 ± 10 % ($p < 0.0001$).